NATIONAL ADVISORY COMMITTEE FOR AERONAUTICS

TECHNICAL NOTE 3941

COMPARISON OF CALCULATED AND EXPERIMENTAL LOAD DISTRIBUTIONS ON THIN WINGS AT HIGH SUBSONIC AND SONIC SPEEDS

By John L. Crigler

Langley Aeronautical Laboratory
Langley Field, Va.

Washington
January 1957

NATIONAL ADVISORY COMMITTEE FOR AERONA

TECHNICAL NOTE 3941

COMPARISON OF CALCULATED AND EXPERIMENTAL LOAD DISTRIBUTIONS ON THIN WINGS AT HIGH SUBSONIC AND SONIC SPEEDS

By John L. Crigler

SUMMARY

A method for calculating the aerodynamic loading on a wing in combination with a body is presented. The method is similar to that used by Falkner for wings in incompressible flow, except that the present method directly relates the downwash velocity to the lift on the wing in a compressible medium for any Mach number.

Calculated results are compared with experimental data for two wing-body configurations throughout a range of Mach number up to 1.0. Both wings were swept back 45° with an aspect ratio of 4. One of the wings had a taper ratio of 0.6 and NACA 65A006 airfoil sections and was tested with and without twist. The other wing had a taper ratio of 0.15 and NACA 64A206, a = 0 airfoil section at the fuselage boundary, fairing to an NACA 64A203, a = 0.8 (modified) airfoil section at the midspan. The sections of the wing from the midspan to the tip were NACA 64A203, a = 0.8 (modified).

The magnitude and the distribution of spanwise loading of the calculated data are in good agreement with experiment up to a Mach number of 0.95, and for the highly tapered wing the agreement of the calculated spanwise load distribution with the experimental distribution is still good up to a Mach number of 0.98.

INTRODUCTION

In recent years the calculation of span loading on wings for wing-body combinations has become of increasing importance for airplane designers. The great number of airplanes with widely different types of plan form, designed to fly at high Mach numbers, makes it virtually impossible to obtain experimental data on the aerodynamic characteristics

over the complete flight range for all wings of interest. Thus, there has been considerable interest in calculation methods, particularly in the calculation of the distribution, or shape, of the span loading.

The purpose of this report is to show to what degree span load distributions as calculated by linear theory agree with experimentally measured span load distributions, particularly in the speed ranges approaching sonic conditions. In making this study, calculated span load distributions are compared with experimentally measured values for some thin wings for wing-body combinations throughout a Mach number range up to $M_o = 1.0$.

The method used in making the calculations for the present study is similar to that used by Falkner in reference 1 for treating wings in incompressible flow and to that used in reference 2 for treating oscillating finite wings in subsonic compressible flow. The present method directly relates the downwash velocity to the lift on the wing in a compressible medium for any Mach number up to $M = 1.0$. As in Falkner's method for incompressible flow, the loading is assumed to be expressible as the sum of terms involving certain unknown coefficients, appearing in the lift distribution. By assuming the downwash to be known at an appropriate number of points, a system of linear algebraic equations is obtained from which the unknown coefficients can be determined.

In order to calculate the load distributions of the wing in combination with a body use was made of the method suggested in reference 3, wherein the boundary conditions on the fuselage are assumed to be adequately satisfied by a vortex image system.

SYMBOLS

A	aspect ratio, $4s^2/S$
$a_{n,m}$	coefficients in expression for lift
C_L	lift coefficient, L/qS
c	section chord, ft
c_r	root chord, ft
c_{av}	average chord, $\frac{S}{2s}$, ft

c_t	tip chord, ft
c_l	section lift coefficient
c_m	section moment coefficient
D	fuselage diameter, in.
d	arbitrary distance, ft
E	total downwash factor
F, f	downwash factors for trailing vortex
G, g	downwash factors for bound vortex
$G_{n,\nu}$	chordwise replacement load
K	kernel function
L	lift, $\int l\ dy$, lb
l	section lift, $\int \Delta l\ dx$, lb
Δl	lift at any point, lb
M	moment, ft-lb
M_o	free-stream Mach number
m	tangent of angle of sweep of local chord line
m'	tangent of angle of sweep of midchord line
q	dynamic pressure, $\frac{1}{2}\rho V^2$, lb/sq ft
r	radius of an infinite cylinder representing body, ft
$\bar{r}$	dimensionless radius with respect to s_v
S	wing area, sq ft
s	wing semispan, ft
s_v	semispan of vortex

V	airstream velocity, ft/sec
w	induced vertical velocity, ft/sec
X	distance of lift point from midchord line along X-axis, $x_m - x_b$
x,y,z	longitudinal, lateral, and vertical coordinates, respectively
$\bar{x},\bar{y}$	dimensionless coordinates, $\frac{x}{s_v}, \frac{y}{s_v}$
x_m,y_m	coordinates of points along midchord line
$\frac{x_{cp}}{c}$	wing section center of pressure
$\left(\frac{x_{cp}}{c_r}\right)_{wb}$	longitudinal center of pressure for wing-body configuration
α	angle of attack, deg
$\beta = \sqrt{1 - M^2}$	
η	dimensionless coordinate, $\frac{y}{s}$
$\theta = \cos^{-1}\frac{X}{c/2}$	
λ	taper ratio, c_t/c_r
Λ	sweep angle of quarter-chord line, positive for sweepback, deg
ρ	density of air, slugs/cu ft

Subscripts:

a	index of control points
b	index of lift point or vortex

Superscripts:

(i)	downwash factor of image vortex
'	downwash factor of vortex located at point $(x_b,-y_b)$

METHOD

The method used in making the calculations is as follows:

Figure 1 shows a wing diagram and the coordinate system employed. In reference 4 the boundary-value problem for the lift distribution on a finite wing is reduced to an integral equation of the form:

$$w(x_a,y_a) = \frac{1}{4\pi} \iint_S \Delta l(x_b,y_b) K(x_a - x_b, y_b - y_a) dx_b \, dy_b \qquad (1)$$

In this expression $w(x_a,y_a)$ represents the displacement velocity at any point (x_a,y_a), or the local downwash velocity at point (x_a,y_a), and may be assumed to be known. The value Δl represents the unknown lift distribution and the kernel K represents the known vertical velocity, or downwash, at point (x_a,y_a) associated with a pressure doublet of unit strength located at any other point (x_b,y_b). In the case of incompressible flow, K is found to be a function only of the distances $(x_a - x_b)$ and $(y_b - y_a)$. In the case of compressible flow, K is a function not only of the distances $(x_a - x_b)$ and $(y_b - y_a)$ but also of the Mach number M_o. The integral equation for this case may be written as (see eq. (15), ref. 4)

$$w(x_a,y_a) = -\frac{1}{4\pi} \iint_S \Delta l(x_b,y_b) \frac{1}{(y_b - y_a)^2} \left[1 + \frac{x_a - x_b}{\sqrt{(x_a - x_b)^2 + \beta^2 (y_b - y_a)^2}} \right] dx_b \, dy_b \qquad (2)$$

where S denotes the surface of the wing projected on the xy-plane. The problem now is to determine $\Delta l(x_b,y_b)$ so as to satisfy equation (2). For arbitrary wings, it does not appear possible to obtain exact solutions to this integral equation; therefore, approximate methods must be resorted to. The method employed is to assume that the lift $\Delta l(x_b,y_b)$ can be expressed in the form of a series of loading terms having both spanwise and chordwise variables, as

$$\Delta l\left(x_b,y_b\right) = \frac{8\rho V^2}{c}\tan\alpha\sqrt{s^2-y_b^2}\left[\cot\frac{\theta}{2}\left(a_{0,0}+\frac{y_b}{s}a_{0,1}+\frac{y_b^2}{s^2}a_{0,2}+\cdots\right)+\right.$$

$$\sin\theta\left(a_{1,0}+\frac{y_b}{s}a_{1,1}+\frac{y_b^2}{s^2}a_{1,2}\cdots\right)+$$

$$\left.\sin 2\theta\left(a_{2,0}+\frac{y_b}{s}a_{2,1}+\frac{y_b^2}{s^2}a_{2,2}\mp\cdots\right)\cdots\right] \qquad (3)$$

where

$$\cos\theta = \frac{x_m - x_b}{c/2} = \frac{X}{c/2} \qquad \left(0\leqq\theta\leqq\pi\right)$$

as shown in figure 1. The value $\theta = 0$ corresponds to points on the wing leading edge and $\theta = \pi$ corresponds to points on the wing trailing edge.

In equation (3), s denotes the semispan of the wing so that this expression for the lift denotes an elliptic type of loading with modifications given in terms of the variable y_b. The first term of the distribution, $\cot\frac{\theta}{2}$, implies a $\frac{1}{\sqrt{x}}$ type of singularity at the wing leading edge, and each term of the series goes continuously to zero at the wing trailing edge. Substituting the expression for the lift given in equation (3) into the integral equation (2) expresses the total local downwash $w\left(x_a,y_a\right)$ as a sum of terms involving the coefficients $a_{n,m}$ as the unknowns with all other quantities in the equation known. For example,

$$w\left(x_a,y_a\right) = -\frac{\rho V^2}{\pi}\tan\alpha\int_{-s}^{s}\sqrt{b^2-y_b^2}\,dy_b\int_0^{\pi}\left[\cot\frac{\theta}{2}\left(a_{0,0}+\frac{y_b}{s}a_{0,1}+\frac{y_b^2}{s^2}a_{0,2}+\cdots\right)+\right.$$

$$\sin\theta\left(a_{1,0}+\frac{y_b}{s}a_{1,1}+\frac{y_b^2}{s^2}a_{1,2}+\cdots\right)+\sin 2\theta\left(a_{2,0}+\frac{y_b}{s}a_{2,1}+\right.$$

$$\left.\left.\frac{y_b^2}{b^2}a_{2,2}+\cdots\right)\right]\frac{1}{\left(y_b-y_a\right)^2}\left[1+\frac{x_a-x_b}{\sqrt{\left(x_a-x_b\right)^2+\beta^2\left(y_b-y_a\right)^2}}\right]\sin\theta\,d\theta$$

or

$$w(x_a,y_a) = -\frac{\rho V^2 s^2 \tan\alpha}{\pi}\int_{-1}^{1}\sqrt{1-\eta^2}\,d\eta\int_0^{\pi}\Bigg[\cot\frac{\theta}{2}\left(a_{0,0}+\eta a_{0,1}+\eta^2 a_{0,2}+\cdots\right)+$$

$$\sin\theta\left(a_{1,0}+\eta a_{1,1}+\eta^2 a_{1,2}+\cdots\right)+\sin 2\theta\left(a_{2,0}+\eta a_{2,1}+$$

$$\eta^2 a_{2,2}+\cdots\right)\cdots\Bigg]\frac{1}{(y_b-y_a)^2}\left[1+\frac{x_a-x_b}{\sqrt{(x_a-x_b)^2+\beta^2(y_b-y_a)^2}}\right]\sin\theta\,d\theta \qquad (4)$$

where

$$\eta = \frac{y_b}{s}$$

The problem now is to evaluate the integrals in equation (4) in order to determine the coefficients $a_{n,m}$. It should be noted, however, that equation (4) consists of a series of elliptic integrals which cannot be evaluated in closed form. The integrals can nevertheless be accurately performed by approximate or numerical procedures for any preassigned values of (x_a,y_a). Since the total downwash velocity $w(x_a,y_a)$ is assumed to be known, it may be seen that the integrations yield equations for $w(x_a,y_a)$ in terms of the unknown coefficients $a_{n,m}$ appearing in the lift distribution. Thus, by assuming the downwash velocity to be known at an appropriate number of points, called "control points," a system of linear algebraic equations is obtained from which the coefficients $a_{n,m}$ can be determined. It is significant to note that, when a is determined, the lift is expressed in a perfectly continuous form except for the allowable singularity along the leading edge.

The Spanwise Integration of the Downwash

In evaluating the integrals in equation (4), either the chordwise or the spanwise integration may be performed first. The procedure herein begins with the spanwise integration; that is, with an evaluation of the integral

$$\frac{dw}{d\theta}(x_a,y_a) = \sin\theta \frac{1}{4\pi}\int_{-s}^{s} \Delta l(\theta,y_b)K(x_a,y_a, M_o, \theta, y_b)\,dy_b \qquad (5)$$

where x_a, y_a, M_o, and θ are assumed to be fixed. In order to evaluate the integral along a curve of constant θ, let this curve be divided into small arc lengths Δd by dividing the span length $2s$ into small elements of span, of width $2s_v$, and let x_μ, y_μ represent the midpoint of the μth span element as indicated in the following sketch.

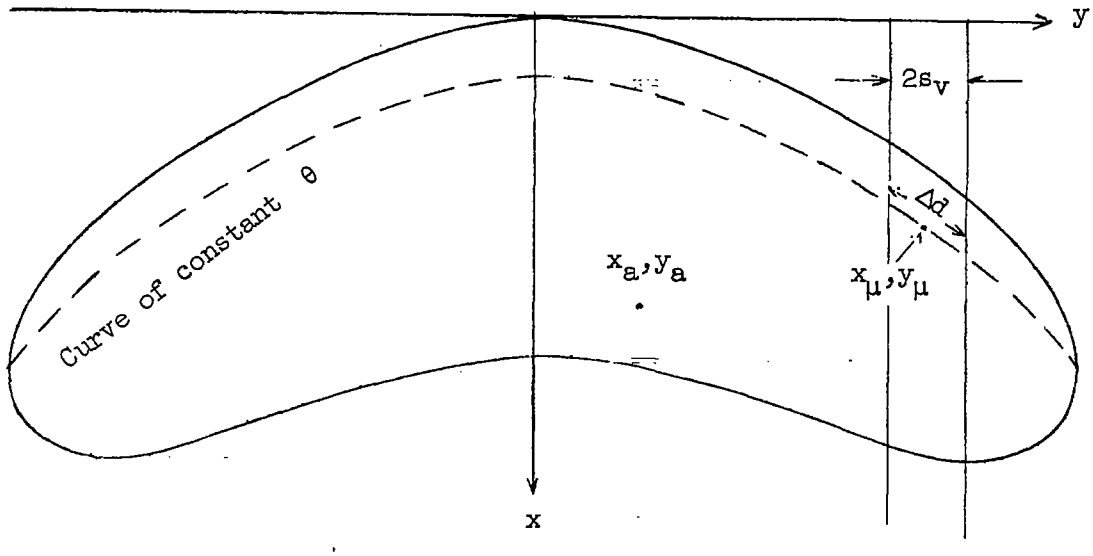

The integral, equation (5), may now be written as a sum of integrals,

$$\frac{dw}{d\theta}(x_a,y_a) = \frac{1}{4\pi}\sin\theta \sum_{\mu=1}^{s/s_v} \int_{y_\mu - s_v}^{y_\mu + s_v} \Delta l(\theta,y_b)K(x_a,y_a, M_o, \theta, y_b)\,dy_b \qquad (6)$$

The approximation is made on the assumption that the element of span of width $2s_v$ can be taken small enough, compared with the semispan s,

that the value of the loading $\Delta l(\theta, y_\mu)$ at the midpoint of the element adequately represents the value at any point of the element. This spanwise approximation may be carried out to any desired degree of accuracy so that in the limit the feature of a continuous load distribution is retained.

Thus, the value of $\frac{dw}{d\theta}$ may be approximately written as

$$\frac{dw}{d\theta}(x_a,y_a) \approx \frac{1}{4\pi} \sum_{\mu=1}^{s/s_v} 2s_v \Delta l(\theta, y_\mu) E\left(\overline{x_a}, M_o, \theta, \overline{y_\mu}-\overline{y_a}\right) \sin\theta \tag{7}$$

where

$$E\left(\overline{x_a}, M_o, \theta, \overline{y_\mu}-\overline{y_a}\right) = \int_{y_\mu-s_v}^{y_\mu+s_v} K(x_a,y_a, M_o, \theta, y_b)\, dy_b \tag{8}$$

The integration required to obtain the function E in explicit form can readily be carried out with the results expressed in terms of the distances $(x_a - x_\mu)$ and $(y_\mu - y_a)$ and the free-stream Mach number M_o. (See, for example, ref. 5 where the expression for E is derived by using a different notation.) The value of E is identical with the downwash function associated with a horseshoe vortex where the bound leg is of length $2s_v$ with its midpoint located at x_μ, y_μ. As will be discussed later, it is necessary to apply a correction to the downwash due to the bound leg of the horseshoe vortex to account for the increase in vertical velocity caused by the fuselage. For this reason the contributions associated with the bound legs and trailing legs are employed separately. The derivation of E in this separated form is given in appendix A.

The Chordwise Integration of the Downwash

After having performed the spanwise integration, the next step is to effect the chordwise integration; that is,

$$w(x_a,y_a) = \frac{1}{4\pi} 2s_v \sum_{\mu=1}^{s/s_v} \int_0^\pi \Delta l(\theta, y_\mu) E\left(\overline{x_a}, M_o, \theta, \overline{y_\mu}-\overline{y_a}\right) \sin\theta \, d\theta \tag{9}$$

It must be remembered that the lift distribution given by $\Delta l(\theta, y_\mu)$ in equation (9) is an unknown quantity, involving certain coefficients $a_{n,m}$ which have to be determined. The integrations in equation (9) may be effected by evaluating the integrand for fixed values of x_a, y_a, M_o, and y_μ at small intervals of θ and then making use of some curve-fitting scheme of integration such as Simpson's rule. It should be noted, however, that since E is equivalent to the downwash function associated with a horseshoe vortex, equation (9) is the basic equation of Falkner's procedure for treating the lifting surface. Falkner, in lieu of using small spacings in the chordwise direction, devised a scheme to approximate the integration that involves evaluating the integrand in equation (9) for only a few discrete values of θ. Falkner used the method for the case of a steady wing in incompressible flow, but the method can easily be extended to steady wings in compressible flow and to oscillating wings in either compressible or incompressible flow. (See, for example, ref. 2.) The method of chordwise integration, as devised by Falkner, consists of expressing $\Delta l(\theta, y_\mu)$ in terms of $a_{n,m}$ for only a few discrete values of θ, denoted herein by θ_ν ($\nu = 1, 2, 3, \ldots Q$) and employing weighting factors $G_{n,\nu}$ associated with each value of ν. Although there is no apparent justification for using this method of chordwise integration for $M_o = 1$, calculations have been made for this condition herein.

The method of determining the weighting factors $G_{n,\nu}$ is discussed in the next section.

It is convenient to locate the control points so that they fall along fixed percentage span and chord positions; that is, along constant η and constant θ curves. The spanwise locations of control points are chosen so that they lie midway between the legs of the horseshoe vortex. The chordwise locations are chosen so that the control points fall midway between the lines of constant θ, which means there must be at least one more discrete value of θ than chordwise control points. Since one equation is formed at each control point there should be the same number of control points as coefficients $a_{n,m}$ retained in the equation for lift. In the present treatment, the number of both spanwise and chordwise control points are made to equal the number of spanwise and chordwise terms retained in the series, nine.

Now, at any control point with coordinates x_a, y_a, let $G_{n,\nu}$ represent the weighting factor for the nth term of the spanwise loading distribution and the νth value of θ. The μth integral in equation (9) may then be written

$$w(x_a,y_a) = \frac{1}{4\pi} 2s_v \int_0^\pi \Delta l\,(\theta, y_\mu)\, E(\overline{x_a}, M_o, \theta, \overline{y_\mu - y_a}) \sin\theta\, d\theta$$

$$\approx \frac{1}{4\pi} 2s_v \sum_{\nu=1}^{Q} \sum_{n=0}^{R} G_{n,\nu} s \sqrt{1-\eta^2} \left(a_{n,0} + a_{n,1}\eta + \ldots + a_{n,m}\eta^m\right) E(\overline{x_a}, M_o, \theta_\nu, \overline{y_\mu - y_a}) \quad (10)$$

Determination of the Weighting Factors

The weighting factors $G_{n,\nu}$ are determined with the use of theory for a two-dimensional wing by setting up a system of algebraic equations for the lift and the downwash involving these factors. Each chordwise term in the lift series requires a system of equations; but each set of equations is obtained in the same manner. The details are therefore presented only for the $n = 0$ term; that is, for the term containing $\cot \frac{\theta}{2}$.

The first equation to be considered equates the integral of the continuous loading to the sum of the weighting factors; namely,

$$\sum_{\nu=1}^{Q} G_{0,\nu} = G_{0,1} + G_{0,2} + \cdots + G_{0,Q} = \int_0^{\pi} \cot \frac{\theta}{2} \sin \theta \, d\theta = \frac{\pi}{2} \qquad (11)$$

Each of the other $(Q - 1)$ equations in the system involves one chordwise location of control point (midway between lines of constant θ) and all the discrete values of θ. These equations are derived by the use of the two-dimensional kernel or downwash function. The downwash at the control point involved, as produced by the sum of the loads on each discrete value of θ is equated to the downwash produced by the continuous loading in two-dimensional flow; that is, if $x_1, x_2, \cdots x_{(Q-1)}$ denotes the $(Q - 1)$ chordwise control-point location (x is midway between lines of constant θ), then for $x = x_1$

$$\sum_{\nu=1}^{Q} G_{0,\nu} K(x_1, M_o, \theta_\nu) = G_{0,1} K(x_1, M_o, \theta_1) + G_{0,2} K(x_1, M_o, \theta_2) + \cdots + G_{0,Q} K(x_1, M_o, \theta_m)$$

$$= \int_0^{\pi} K(x_1, M_o, \theta) \cot \frac{\theta}{2} \sin \theta \, d\theta$$

$$= \pi\beta \qquad (12)$$

These equations are independent of Mach number and, therefore, are identical to the equations for the incompressible case. The weighting factors for various values of θ_ν have been tabulated. (For example, see ref. 1.)

The equations for the first term of the lift series (the term containing $\cot\frac{\theta}{2}$) for four values of θ corresponding to the 12.5-, 37.5-, 62.5-, and 87.5-percent-chord lines are

$$\left.\begin{aligned} G_{0,1} + G_{0,2} + G_{0,3} + G_{0,4} &= \frac{\pi}{2} \\ 8G_{0,1} - 8G_{0,2} - \frac{8}{3}G_{0,3} - \frac{8}{5}G_{0,4} &= \pi \\ \frac{8}{3}G_{0,1} + 8G_{0,2} - 8G_{0,3} - \frac{8}{3}G_{0,4} &= \pi \\ \frac{8}{5}G_{0,1} + \frac{8}{3}G_{0,2} + 8G_{0,3} - 8G_{0,4} &= \pi \end{aligned}\right\} \tag{13}$$

Similarly, four equations to determine $G_{n,\nu}$ for any other value of n are obtained by replacing the load term containing $\cot\frac{\theta}{2}$ in equation (11) by the term containing $\sin n\theta$. The weighting factors are tabulated in table I for four values of θ corresponding to the 12.5-, 37.5-, 62.5-, and 87.5-percent-chord lines.

Determination of the Downwash

After $G_{n,\nu}$ is determined for a given choice of θ-values, the expression for the total downwash at any particular control point is given with the use of equations (9) and (10) as

$$w(x_a,y_a) = \frac{1}{4\pi} 2s_v \sum_{\mu=1}^{s/s_v} \sum_{\nu=1}^{Q} \sum_{n=0}^{R} G_{n,\nu} s\sqrt{1-\eta^2}\left(a_{n,0} + a_{n,1}\eta + \cdots + a_{n,m}\eta^m\right) E\left(\overline{x_a}, M_0, \theta_\nu, \overline{y_\mu - y_a}\right) \tag{14}$$

Since the total downwash is known at the chosen control points, equation (14) leads to a system of linear algebraic equations from which the coefficient $a_{n,m}$ can be determined.

An example showing the formation of the downwash equations for the 84-vortex pattern with four θ-lines is given in appendix B.

Effect of Presence of Fuselage

In the analytical treatment of the wing-fuselage combination, the fuselage is represented by an infinite cylinder, which is replaced by the images of the wing vortices placed inside the fuselage as suggested in reference 3. As indicated in reference 3, the boundary conditions are satisfied exactly only infinitely far behind the wing. The vortices used to represent the fuselage induce a downwash on the wing which must be taken into account. This additional downwash may be approximated by a correction to the downwash due to the bound vortices as discussed in reference 3. The corrected downwash is then given as

$$\text{Corrected downwash} = \text{Downwash}\left(1 + \frac{\bar{r}^2}{\bar{y}_a^2}\right)$$

MODELS

Calculations have been made for two wing-body configurations. One wing, designated wing A, was swept back 45°, with an aspect ratio of 4, a taper ratio of 0.6, and NACA 65A006 airfoil sections parallel to the plane of symmetry. Details of wing A in combination with the body are given in figure 2. Experimental data used in the comparisons for wing A were obtained from tests made in the Langley 8-foot transonic tunnel. Both experimental and calculated results were obtained for this wing without twist and for the wing with a spanwise twist variation from the fuselage boundary to the wing tip as shown in figure 3. This spanwise variation was produced by twisting the wing sections about the wing quarter-chord line in planes parallel to the vertical plane of symmetry. In making the calculations the body in all cases was treated as an infinite cylinder, as indicated by the dashed lines in figure 2.

The other wing, designated wing B, was swept back 45°, with an aspect ratio of 4, a taper ratio of 0.15, and NACA 64A206, a = 0 airfoil sections at the wing midspan, fairing into NACA 64A203, a = 0.8 (modified) airfoil sections at the 0.5 semispan and retaining these sections from the midspan to the wing tip. Details of wing B in combination with the body are given in figure 4. These calculated data are compared with unpublished experimental data obtained in the Langley 8-foot transonic tunnel.

COMPARISON OF EXPERIMENTAL AND CALCULATED RESULTS

Figure 5 shows a comparison of the calculated spanwise loading of wing A alone with that of the same wing in combination with a body. The details of the wing-body configuration are shown in figure 2. The calculations are for an angle of attack of 4.0°. Figure 5(a) shows the results for incompressible flow ($M_0 = 0$) and figure 5(b) shows the results for compressible flow for $M_0 = 0.9$. The only significant effect of the body is to reduce the loading on the wing adjacent to the body and for these two cases the effect was less at $M_0 = 0.9$ than for the incompressible flow case. The loadings on the more important outboard sections are not significantly affected. In all remaining calculations the effect of the body is included for comparison with experimentally measured data since no experimental data have been obtained with the wing alone. For these and all subsequent calculations, the wing is assumed to have a fixed geometry; that is, no deflection or bending under load. For the wings tested in this report, deflections under load were very small at $\alpha = 4.0^\circ$, so that any discrepancies introduced in the calculations due to deflection or bending were small. However, in many cases, this effect is important, and if so, must be included in the calculations.

Figure 6 shows a comparison of the calculated and experimentally measured spanwise loading plotted against the wing semispan for Mach numbers of 0.6, 0.95, and 1.0 for wing A in combination with a body. The data are for an angle of attack of 4.0° and for the wing without twist. The spanwise distribution of lift, on which the wing spanwise shears and bending moments depend, are generally in good agreement, both in shape and magnitude. It may be noted that, for $M_0 = 1.0$, there is a drop in the measured lift adjacent to the body and also an increase near the tip which results in a change in the shape of the loading curve; that is, an outward shift in the lateral center of pressure which is not found in the calculated results.

Figure 7 shows a comparison of results for the same wing-body configuration and the same Mach number range as shown in figure 6; however, in this case the wing sections were twisted about the quarter-chord line to produce the spanwise twist variation shown in figure 3. These data are also for an angle of attack of 4.0°, the angle of attack being measured from the body center line. The agreement of theory and experiment, here again, is good and the same trends with Mach number as in figure 6 are noted. It thus appears that the changes in span loading which result from twisting due to aeroelastic bending or wing deflections can be predicted at these Mach numbers.

Figure 8 shows calculated and experimental spanwise loading coefficients for wing B. The details of the wing-body configuration are shown in figure 4. The results are for an angle of attack of 4.0° and are shown

for Mach numbers of 0.80, 0.94, 0.98, and 1.0. The agreement between theory and experiment for Mach numbers of 0.80 and 0.94 shown in figure 8(a) and for $M_o = 0.98$ shown in figure 8(b) is very good. This wing was not tested at a Mach number of 1.0, the highest Mach number for which calculations have been made, but experimentally measured data were obtained at $M_o = 1.03$. These experimental data fell below the curve for $M_o = 0.98$ and there was no appreciable difference between the experimental data for $M_o = 0.94$ and $M_o = 0.98$. The shape or distribution of the loading for the calculated data at $M_o = 1.0$ was essentially in agreement with the distribution of the experimental curves for $M_o = 0.98$ and $M_o = 1.03$. Thus it appears that for this wing there is a an appreciable increase in the magnitude of the loading on going from $M_o = 0.98$ to $M_o = 1.0$ for the calculated data that would not be found experimentally.

For the cases that have been calculated it may be concluded that the magnitude and the distribution of spanwise loading calculated for the thin wings under consideration are in good agreement with experiment up to a Mach number of 0.95, and for the highly tapered wing (wing B) the agreement is still good up to a Mach number of 0.98.

Figure 9 shows a comparison of the calculated and experimentally measured chordwise center-of-pressure location for several spanwise sections for wing A over the range of Mach number tested and figure 10 shows similar results for wing B. The experimental data in figure 9(a) for the untwisted wing for $M_o = 0.8$ and $M_o = 0.9$ were taken from reference 6. On both wings the agreement over the inboard section is good up to a Mach number of 1.0. However, there is a sharp rearward shift in the chordwise center of pressure location shown at the 0.8 and 0.95 semispan stations for the experimental data occurring between $M_o = 0.95$ and $M_o = 1.0$ that is not indicated by the calculated data. With regard to the chordwise pressure distribution good correlation would not be expected, particularly over the outboard sections where there might be a tendency for the flow to wash out towards the tip.

Figure 11(a) shows a comparison of the calculated and experimental longitudinal center-of-pressure location relative to the leading edge of the root chord versus Mach number for wing A with body without twist. The calculated data are for a constant angle of attack of 4.0°. The calculated lift coefficients, varying from $C_L = 0.260$ at $M_o = 0.8$ to $C_L = 0.306$ at $M_o = 1.0$ are shown on the figure. The experimental data are for lift coefficients of 0.2 and 0.4. The calculated longitudinal center of pressure for the wing-body combination is approximately at the trailing edge of the root chord for this wing without twist and is seen to shift slightly rearward with an increase in Mach number. The shift in the longitudinal center of pressure for the experimental data is somewhat greater as M_o approaches 1.0. This greater shift in the

longitudinal center of pressure for the complete wing would be expected from the sharp rearward shift in the chordwise center-of-pressure location for the outboard sections shown in figure 9.

Figure 11(b) shows a comparison similar to figure 11(a) for wing A with body and with twist in the wing. Again the calculated data are for a constant angle of attack of 4.0° and the calculated lift coefficients for several Mach numbers are shown. In general, the same trends are shown, except in this case the longitudinal center-of-pressure location for the experimental data at $C_L = 0.4$ was about 7 percent of the root chord behind that for a C_L of 0.2. Other experimental data for this configuration, not presented herein, showed no appreciable shift in the center-of-pressure locations for lift coefficients of 0.6 and 0.8 from that at $C_L = 0.4$.

Figure 12 shows a comparison of the calculated and experimental longitudinal center-of-pressure location relative to the leading edge of the root chord against Mach number for wing B. The calculated data are for a constant angle of attack of 4.0°. The experimental data are only given for a lift coefficient of 0.4 since the calculated lift coefficients were near 0.4. The same trends as noted in figure 11 are shown for this wing-body combination.

CONCLUDING REMARKS

A detailed method for calculating the span load distribution of a wing in combination with a body is presented. A comparison of the calculated load distributions with experimental results indicated that, for the limited number of cases calculated, the magnitude and distribution of spanwise loading calculated for these thin wings are in good agreement with experiment up to a Mach number of 0.95 and that the spanwise loading calculated for the highly tapered wing is in good agreement with experiment up to a Mach number of 0.98.

Langley Aeronautical Laboratory,
National Advisory Committee for Aeronautics,
Langley Field, Va., June 11, 1956.

APPENDIX A

DERIVATION OF DOWNWASH FACTOR E

It was pointed out in the text of the report that the method of effecting the spanwise integration of loading employed led to a system of horseshoe vortices. From considerations in reference 3, the wing-body combination is represented by a set of vortices located on the wing with image vortices located inside the body. Since a correction is applied to the downwash associated with the leg of the vortex, as outlined in reference 3, it is desirable to calculate the contribution due to the trailing legs and bound leg separately. The downwash in this separated form is calculated with the use of the Biot-Savart law.

The contribution of the trailing legs of the vortex at (x_b,y_b) and of width $2s_v$ to the downwash factor at point (x_a,y_a) is given by

$$f_{b,a} = \frac{1}{y_b - y_a + s_v}\left[\frac{(x_a - x_b) + \sqrt{(x_a - x_b)^2 + \beta^2(y_b - y_a + s_v)^2}}{\sqrt{(x_a - x_b)^2 + \beta^2(y_b - y_a + s_v)^2}}\right] - \frac{1}{y_b - y_a - s_v}\left[\frac{(x_a - x_b) + \sqrt{(x_a - x_b)^2 + \beta^2(y_b - y_a - s_v)^2}}{\sqrt{(x_a - x_b)^2 + \beta^2(y_b - y_a - s_v)^2}}\right] \tag{A1}$$

or referring all distances to the vortex semispan s_v

$$f_{b,a} = \frac{1}{\bar{y}_b - \bar{y}_a + 1}\frac{1}{s_v}\left[\frac{(\bar{x}_a - \bar{x}_b) + \sqrt{(\bar{x}_a - \bar{x}_b)^2 + \beta^2(\bar{y}_b - \bar{y}_a + 1)^2}}{\sqrt{(\bar{x}_a - \bar{x}_b)^2 + \beta^2(\bar{y}_b - \bar{y}_a + 1)^2}}\right] - \frac{1}{\bar{y}_b - \bar{y}_a - 1}\frac{1}{s_v}\left[\frac{(\bar{x}_a - \bar{x}_b) + \sqrt{(\bar{x}_a - \bar{x}_b)^2 + \beta^2(\bar{y}_b - \bar{y}_a - 1)^2}}{\sqrt{(\bar{x}_a - \bar{x}_b)^2 + \beta^2(\bar{y}_b - \bar{y}_a - 1)^2}}\right] \tag{A2}$$

The contribution of the bound leg of the vortex at (x_b,y_b) and of width $2s_v$ to the downwash factor at point x_a,y_a which is increased by the factor $\left(1 + \frac{r^2}{y^2}\right)$ (see ref. 2) is given by

$$g_{b,a} = \frac{\beta^2}{\bar{x}_a - \bar{x}_b} \frac{1}{s_v} \left[\frac{\bar{y}_b - \bar{y}_a + 1}{\sqrt{(\bar{x}_a - \bar{x}_b)^2 + \beta^2(\bar{y}_b - \bar{y}_a + 1)^2}} - \frac{\bar{y}_b - \bar{y}_a - 1}{\sqrt{(\bar{x}_a - \bar{x}_b)^2 + \beta^2(\bar{y}_b - \bar{y}_a - 1)^2}} \right] \tag{A3}$$

The contribution to the downwash factor at point (x_a, y_a) due to the vortex at $(x_b, -y_b)$ for a wing with symmetrical loading, $\Delta l(x_b, y_b) = \Delta l(x_b, -y_b)$, is given by

$$f'_{b,a} = \frac{1}{\bar{y}_b + \bar{y}_a + 1} \frac{1}{s_v} \left[\frac{(\bar{x}_a - \bar{x}_b) + \sqrt{(\bar{x}_a - \bar{x}_b)^2 + \beta^2(\bar{y}_b + \bar{y}_a + 1)^2}}{\sqrt{(\bar{x}_a - \bar{x}_b)^2 + \beta^2(\bar{y}_b + \bar{y}_a + 1)^2}} \right] - \frac{1}{\bar{y}_b + \bar{y}_a - 1} \frac{1}{s_v} \left[\frac{(\bar{x}_a - \bar{x}_b) + \sqrt{(\bar{x}_a - \bar{x}_b)^2 + \beta^2(\bar{y}_b + \bar{y}_a - 1)^2}}{\sqrt{(\bar{x}_a - \bar{x}_b)^2 + \beta^2(\bar{y}_b + \bar{y}_a - 1)^2}} \right] \tag{A4}$$

and

$$g'_{b,a} = \frac{\beta^2}{\bar{x}_a - \bar{x}_b} \frac{1}{s_v} \left[\frac{\bar{y}_b + \bar{y}_a + 1}{\sqrt{(\bar{x}_a - \bar{x}_b)^2 + \beta^2(\bar{y}_b + \bar{y}_a + 1)^2}} - \frac{\bar{y}_b + \bar{y}_a - 1}{\sqrt{(\bar{x}_a - \bar{x}_b)^2 + \beta^2(\bar{y}_b + \bar{y}_a - 1)^2}} \right] \tag{A5}$$

Each discrete vortex located on the wing is considered to have an image vortex of the same strength inside the fuselage that must be considered in summing up the downwash at any control point. A horseshoe vortex of width $y_2 - y_1$ located outside of a cylinder of radius r has an image horseshoe vortex of width $\left(\frac{r^2}{y_1} - \frac{r^2}{y_2}\right)$ within the cylinder. Then the contribution to the downwash factor at point (x_a, y_a) due to the image inside the fuselage of the vortex at x_b, y_b is given by

$$f_{b,a}^{(i)} = \frac{1}{\bar{y}_a - \frac{\bar{r}^2}{\bar{y}_b + 1}} \frac{1}{s_v}\left[\frac{(\bar{x}_a - \bar{x}_b) + \sqrt{(\bar{x}_a - \bar{x}_b)^2 + \beta^2\left(\bar{y}_a - \frac{\bar{r}^2}{\bar{y}_b + 1}\right)^2}}{\sqrt{(\bar{x}_a - \bar{x}_b)^2 + \beta^2\left(\bar{y}_b - \frac{\bar{r}^2}{\bar{y}_b + 1}\right)^2}}\right] -$$

$$\frac{1}{\bar{y}_a - \frac{\bar{r}^2}{\bar{y}_b - 1}} \frac{1}{s_v}\left[\frac{(\bar{x}_a - \bar{x}_b) + \sqrt{(\bar{x}_a - \bar{x}_b)^2 + \beta^2\left(\bar{y}_a - \frac{\bar{r}^2}{\bar{y}_b - 1}\right)^2}}{\sqrt{(\bar{x}_a - \bar{x}_b)^2 + \beta^2\left(\bar{y}_b - \frac{\bar{r}^2}{\bar{y}_b - 1}\right)^2}}\right] \tag{A6}$$

and

$$g_{b,a}^{(i)} = \frac{\beta^2}{(\bar{x}_a - \bar{x}_b)} \frac{1}{s_v}\left[\frac{\bar{y}_a - \frac{\bar{r}^2}{\bar{y}_b + 1}}{\sqrt{(\bar{x}_a - \bar{x}_b)^2 + \beta^2\left(\bar{y}_a - \frac{\bar{r}^2}{\bar{y}_b + 1}\right)^2}} - \frac{\bar{y}_a - \frac{\bar{r}^2}{\bar{y}_b - 1}}{\sqrt{(\bar{x}_a - \bar{x}_b)^2 + \beta^2\left(\bar{y}_a - \frac{\bar{r}^2}{\bar{y}_b - 1}\right)^2}}\right] \tag{A7}$$

The contribution to the downwash factor at point x_a, y_a due to the image inside the fuselage of the vortex at $x_b, -y_b$ is given by

$$f_{b,a}^{(i)'} = \frac{1}{\bar{y}_a + \frac{\bar{r}^2}{\bar{y}_b - 1}} \frac{1}{s_v}\left[\frac{(\bar{x}_a - \bar{x}_b) + \sqrt{(\bar{x}_a - \bar{x}_b)^2 + \beta^2\left(\bar{y}_a + \frac{\bar{r}^2}{\bar{y}_b - 1}\right)^2}}{\sqrt{(\bar{x}_a - \bar{x}_b)^2 + \beta^2\left(\bar{y}_a + \frac{\bar{r}^2}{\bar{y}_b - 1}\right)^2}}\right] -$$

$$\frac{1}{\bar{y}_a + \frac{\bar{r}^2}{\bar{y}_b + 1}} \frac{1}{s_v}\left[\frac{(\bar{x}_a - \bar{x}_b) + \sqrt{(\bar{x}_a - \bar{x}_b)^2 + \beta^2\left(\bar{y}_a + \frac{\bar{r}^2}{\bar{y}_b + 1}\right)^2}}{\sqrt{(\bar{x}_a - \bar{x}_b)^2 + \beta^2\left(\bar{y}_a + \frac{\bar{r}^2}{\bar{y}_b + 1}\right)^2}}\right] \tag{A8}$$

and

$$g_{b,a}^{(i)'} = \frac{\beta^2}{\bar{x}_a - \bar{x}_b} \frac{1}{s_v} \left[\frac{\bar{y}_a + \frac{\bar{r}^2}{\bar{y}_b - 1}}{\sqrt{\left(\bar{x}_a - \bar{x}_n\right)^2 + \beta^2 \left(\bar{y}_a + \frac{\bar{r}^2}{\bar{y}_b - 1}\right)^2}} - \frac{\bar{y}_a + \frac{\bar{r}^2}{\bar{y}_b + 1}}{\sqrt{\left(\bar{x}_a - \bar{x}_b\right)^2 + \beta^2 \left(\bar{y}_a + \frac{\bar{r}^2}{\bar{y}_b + 1}\right)^2}} \right] \tag{A9}$$

The total downwash factor at point x_a,y_a due to the vortex at x_b,y_b, its companion vortex at $x_b,-y_b$ (on a symmetrical wing), and their images inside the fuselage are given by

$$E = F_{b,a} + G_{b,a}\left(1 + \frac{\bar{r}^2}{\bar{y}_a^2}\right) \tag{A10}$$

where

$$F_{b,a} = f_{b,a} + f_{b,a}' + f_{b,a}^{(i)} + f_{b,a}^{(i)'}$$

and

$$G_{b,a} = g_{b,a} + g_{b,a}' + g_{b,a}^{(i)} + g_{b,a}^{(i)'}$$

APPENDIX B

APPROXIMATE INTEGRATION IN THE CHORDWISE DIRECTION AND FORMATION OF THE DOWNWASH EQUATIONS

In the formation of the downwash equation, there must be one control point for each equation. The location of the control points on the wing depends on the layout used, and the number and optimum locations of the points must be determined by experience. Falkner found the 84-vortex pattern with nine control points located as shown in figure 13 to be satisfactory in computing the load distribution of a symmetrical swept-back wing in incompressible flow with the 328-vortex pattern giving only slightly better accuracy. Therefore, the 84-vortex pattern, or the equivalent, for the wing-body combination which divides the wing into intervals of 0.1 semispan and four chordwise load lines has been used for all calculations in this report. It should be noted, however, that it is quite probable that placing the control points nearer the trailing edge would give better results, particularly as $M_o \longrightarrow 1.0$. Both the spanwise and chordwise distribution of control points are the same as the spanwise and chordwise terms retained in the equations.

The equations for determining $a_{n,m}$ are formed as follows:

The coefficient for $a_{0,0}$ corresponding to the $\cot \frac{\theta}{2}$ term for the 84-vortex solution (control point 1, fig. 11) is given by (see table I for values of $G_{n,\nu}$)

$$0.2734 \sum E_{1/8} \sqrt{1 - \eta^2} + 0.1172 \sum E_{3/8} \sqrt{1 - \eta^2}$$

$$0.0703 \sum E_{5/8} \sqrt{1 - \eta^2} + 0.0391 \sum E_{7/8} \sqrt{1 - \eta^2}$$

where the subscripts 1/8, 3/8, 5/8, and 7/8 on the downwash factors refer to the vortices on the 12.5-, 37.5-, 62.5-, and 87.5-percent-chord lines, respectively.

The coefficient for $a_{1,0}$ corresponding to the $\sin\theta$ term is given by

$$0.0488 \sum E_{1/8}\sqrt{1-\eta^2} + 0.0762 \sum E_{3/8}\sqrt{1-\eta^2} +$$

$$0.0762 \sum E_{5/8}\sqrt{1-\eta^2} + 0.0488 \sum E_{7/8}\sqrt{1-\eta^2}$$

The coefficient for $a_{2,0}$ corresponding to the $\sin 2\theta$ term is given by

$$0.0732 \sum E_{1/8}\sqrt{1-\eta^2} + 0.0381 \sum E_{3/8}\sqrt{1-\eta^2} -$$

$$0.0381 \sum E_{5/8}\sqrt{1-\eta^2} - 0.0732 \sum E_{7/8}\sqrt{1-\eta^2}$$

For more than three chordwise control points it would be necessary to include terms of $\sin n\theta$ where $n \rightarrow 2$.

Additional spanwise terms in the equation are determined by adding further spanwise loading functions. The coefficient for $a_{0,2}$ corresponding to the second $\cot\frac{\theta}{2}$ term is given by

$$0.2734 \sum E_{1/8}\eta^2\sqrt{1-\eta^2} + 0.1172 \sum E_{3/8}\eta^2\sqrt{1-\eta^2} +$$

$$0.0703 \sum E_{5/8}\eta^2\sqrt{1-\eta^2} + 0.0391 \sum E_{7/8}\eta^2\sqrt{1-\eta^2}$$

Similarly, the coefficients for the other unknowns corresponding to the $\cot\frac{\theta}{2}$, the $\sin\theta$, and the $\sin 2\theta$ terms are found. For each equation formed the downwash velocity is equated to the local slope of the wing section; that is, w/V is equated to $\tan\alpha$ or, for the wing divided into intervals of 0.1 semispan, each equation is set equal to 0.025 to

allow for the ratio $\frac{2s}{s_v} = 40$. In a similar manner, equations are formed for the other control points, and, for the case of the wing without twist or camber, all equations for all control points are set equal to 0.025. If twist or camber is incorporated in the wing, the constant for each equation will depend on the twist or camber at the particular control point; that is, the local slope of the wing section.

For the wing-fuselage combination the effective angle of attack must be corrected due to the vertical velocity component induced by the fuselage. If it is assumed that the downwash induced by the bound vortices in the plane of the wing is increased by the factor $1 + \frac{r^2}{y_a^2}$, as in reference 3, the effective angle of attack of the wing is equal to the geometric angle plus the angle induced by the fuselage

$$\alpha_{eff} = \alpha_{geom} + \left(\frac{r}{y_a}\right)^2 \alpha_{fus}$$

or

$$\alpha_{eff} = \alpha_{geom}\left(1 + \frac{r^2}{y_a^2}\right)$$

APPENDIX C

AERODYNAMIC CHARACTERISTICS

The lift (see eq. 3) for any point is given by

$$\Delta l = \frac{8\rho V^2}{c} s \tan \alpha \sqrt{1 - \eta^2} \left[\cot \frac{\theta}{2} \left(a_{0,0} + \eta a_{0,1} + \eta^2 a_{0,2} \cdots \right) + \right.$$

$$\sin \theta \left(a_{1,0} + \eta a_{1,1} + \eta^2 a_{1,2} \cdots \right) +$$

$$\left. \sin 2\theta \left(a_{2,0} + \eta a_{2,1} + \eta^2 a_{2,2} \cdots \right) + \cdots \right] \tag{C1}$$

or the total lift at any chord is

$$l = \frac{8\rho V^2}{c} s \tan \alpha \sqrt{1 - \eta^2} \int_{-c/2}^{c/2} \left[\cot \frac{\theta}{2} \left(a_{0,0} + \eta a_{0,1} + \eta^2 a_{0,2} + \cdots \right) + \right.$$

$$\sin \theta \left(a_{1,0} + \eta a_{1,1} + \eta^2 a_{1,2} + \cdots \right) +$$

$$\left. \sin 2\theta \left(a_{2,0} + \eta a_{2,1} + \eta^2 a_{2,2} + \cdots \right) + \cdots \right] dX \tag{C2}$$

but

$$X = \frac{c}{2} \cos \theta$$

and

$$dX = - \frac{c}{2} \sin \theta \, d\theta$$

Then

$$\int_{-c/2}^{c/2} \cot \frac{\theta}{2} \, dX = - \frac{1}{2} \int_{\pi}^{0} \cot \frac{\theta}{2} \sin \theta \, d\theta = \frac{\pi}{2}$$

$$\int_{-c/2}^{c/2} \sin\theta \, dX = \frac{\pi}{4}$$

and

$$\int_{-c/2}^{c/2} \sin 2\theta \, dX = 0$$

Therefore, equation (C2) for a symmetrical wing becomes

$$l = 8\rho V^2 s \tan\alpha\sqrt{1 - \eta^2}\left[\frac{\pi}{2}\left(a_{0,2} + \eta^2 a_{0,2} + \eta^4 a_{0,4}\right) + \frac{\pi}{4}\left(a_{1,0} + \eta^2 a_{1,2} + \eta^4 a_{1,4}\right)\right] \tag{C3}$$

or the section lift coefficient is

$$c_l = \frac{8\rho V^2 \tan\alpha}{\frac{1}{2}\rho V^2 c} s\sqrt{1 - \eta^2}\,\frac{\pi}{4}\left[2\left(a_{0,0} + \eta^2 a_{0,2} + \eta^4 a_{0,4}\right) + \left(a_{1,0} + \eta^2 a_{1,2} + \eta^4 a_{1,4}\right)\right] \tag{C4}$$

but the total lift on the wing is

$$L = \int_{-s}^{s} l \, dy$$

or

$$C_L = \frac{s\int_{-1}^{1} l \, d\eta}{\frac{1}{2}\rho V^2 S}$$

and

$$\left.\begin{aligned} C_L &= \frac{2s^2}{S} 8 \tan\alpha \int_{-1}^{1} \sqrt{1-\eta^2}\left[\frac{\pi}{2}\left(a_{0,0} + \eta^2 a_{0,2} + \eta^4 a_{0,4}\right) + \right. \\ &\left. \frac{\pi}{4}\left(a_{1,0} + \eta^2 a_{1,2} + \eta^4 a_{1,4}\right)\right] d\eta \\ C_L &= 4A \tan\alpha\left[\frac{\pi}{2}\left(\frac{\pi}{2} a_{0,0} + \frac{\pi}{4} a_{1,0}\right) + \frac{\pi}{8}\left(\frac{\pi}{2} a_{0,2} + \frac{\pi}{4} a_{1,2}\right) + \right. \\ &\left. \frac{\pi}{16}\left(\frac{\pi}{2} a_{0,4} + \frac{\pi}{4} a_{1,4}\right)\right] \end{aligned}\right\} \quad (C5)$$

where

$$A = \frac{4s^2}{S}$$

Then

$$C_L = \frac{A\pi^2 \tan\alpha}{16}\left(16a_{0,0} + 8a_{1,0} + 4a_{0,2} + 2a_{1,2} + 2a_{0,4} + a_{1,4}\right) \quad (C6)$$

The slope of the lift curve is

$$\frac{dC_L}{d\alpha} = \frac{A\pi^2}{16}\left(16a_{0,0} + 8a_{1,0} + 4a_{0,2} + 2a_{1,2} + 2a_{0,4} + a_{1,4}\right) \quad (C7)$$

The ratio of the section lift coefficient c_l at any section y to the total lift coefficient C_L is

$$\begin{aligned} \frac{c_l}{C_L} &= \frac{16s\sqrt{1-\eta^2}}{sc\pi} \\ &= \frac{\left[2\left(a_{0,0} + \eta^2 a_{0,2} + \eta^4 a_{0,4}\right) + \left(a_{1,0} + \eta^2 a_{1,2} + \eta^4 a_{1,4}\right)\right]}{\left[16a_{0,0} + 4a_{0,2} + 2a_{0,4} + 8a_{1,0} + 2a_{1,2} + a_{1,4}\right]} \end{aligned} \quad (C8)$$

The section moment coefficient about the midchord is given by

$$c_m = \frac{4s\pi \tan \alpha}{c^2}\sqrt{1 - \eta^2}\,\frac{c_{av}}{2}\left[1 - (1 - \lambda)\eta\right]\left[\left(a_{0,0} + \eta^2 a_{0,2} + \eta^4 a_{0,4}\right) + \frac{1}{2}\left(a_{2,0} + \eta^2 a_{2,2} + \eta^4 a_{2,4}\right)\right] \tag{C9}$$

and the center of pressure of any section is given by

$$\frac{x_{cp}}{c} = \frac{c_m}{c_l} = \frac{c_{av}}{2c}\,\frac{\left[1 - (1 - \lambda)\eta\right]\left[\left(a_{0,0} + \eta^2 a_{0,2} + \eta^4 a_{0,4}\right) + \frac{1}{2}\left(a_{2,0} + \eta^2 a_{2,2} + \eta^4 a_{2,4}\right)\right]}{\left[2\left(a_{0,0} + \eta^2 a_{0,2} + \eta^4 a_{0,4}\right) + \left(a_{1,0} + \eta^2 a_{1,2} + \eta^4 a_{1,4}\right)\right]} \tag{C10}$$

The moment for the complete wing about a line through the leading edge (x = 0) of the center chord (minor axis) is given by

$$\frac{dM}{\tan \alpha} = 8\rho V^2 s^2 \int_0^1 \left[\left(\frac{c_r}{2} + m'\eta s\right)\sqrt{1 - \eta^2}(\pi)\left(a_{0,0} + \eta^2 a_{0,2} + \eta^4 a_{0,4} + \frac{a_{1,0}}{2} + \eta^2\,\frac{a_{1,2}}{2} + \eta^4\,\frac{a_{1,4}}{2}\right)\right] d\eta -$$

$$8\rho V^2 s^2 \int_0^1 \left\{\frac{c_r}{2}\left[1 - (1 - \lambda)\eta\right]\sqrt{1 - \eta^2}\left(\frac{\pi}{2}\right)\left(a_{0,0} + \eta^2 a_{0,2} + \eta^4 a_{0,4} + \frac{a_{2,0}}{2} + \eta^2\,\frac{a_{2,2}}{2} + \eta^4\,\frac{a_{2,4}}{4}\right)\right\} d\eta \tag{C11}$$

where m' is the tangent of angle of sweep of the midchord line, or

$$\frac{dM}{\tan\alpha} = 4\rho V^2 s^2 \pi^2 c_r \left[\left(\frac{1}{8} + \frac{2}{3}\frac{m's}{\pi c_r} + \frac{1-\lambda}{6\pi}\right)a_{0,0} + \left(\frac{1}{32} + \frac{4}{15}\frac{m's}{\pi c_r} + \frac{1-\lambda}{15\pi}\right)a_{0,2} + \left(\frac{1}{64} + \frac{16}{105}\frac{m's}{\pi c_r} + \frac{4(1-\lambda)}{105\pi}\right)a_{0,4} + \left(\frac{1}{8} + \frac{1}{3}\frac{m's}{\pi c_r}\right)a_{1,0} + \left(\frac{1}{32} + \frac{2}{15}\frac{m's}{\pi c_r}\right)a_{1,2} + \left(\frac{1}{64} + \frac{8}{105}\frac{m's}{\pi c_r}\right)a_{1,4} + \left(\frac{1-\lambda}{12\pi} - \frac{1}{16}\right)a_{2,0} + \left(\frac{1-\lambda}{30\pi} - \frac{1}{64}\right)a_{2,2} + \left(\frac{2(1-\lambda)}{105\pi} - \frac{1}{128}\right)a_{2,4}\right] \tag{C12}$$

but

$$\frac{dL}{d\alpha} = \frac{4s^2}{S}\frac{\pi^2}{16}\frac{1}{2}\rho V^2 S\left(16a_{0,0} + 8a_{1,0} + 4a_{0,2} + 2a_{1,2} + 2a_{0,4} + a_{1,4}\right)$$

$$= \frac{\rho V^2 s^2 \pi^2}{8}\left(16a_{0,0} + 8a_{1,0} + 4a_{0,2} + 2a_{1,2} + 2a_{0,4} + a_{1,4}\right)$$

The longitudinal center of pressure is at

$$\left(\frac{x_{cp}}{c_r}\right)_{wb} = \frac{dM}{dL} = 32c_r\,\frac{k_1a_{0,0} + k_2a_{0,2} + k_3a_{0,4} + k_4a_{1,0} + k_5a_{1,2} + k_6a_{1,4} + k_7a_{2,0} + k_8a_{2,2} + k_9a_{2,4}}{16a_{0,0} + 8a_{1,0} + 4a_{0,2} + 2a_{1,2} + 2a_{0,4} + a_{1,4}} \tag{C13}$$

where

$$k_1 = \frac{1}{8} + \frac{2}{3}\frac{m's}{\pi c_r} + \frac{1-\lambda}{6\pi}$$

and k_2, k_3, k_4, k_5, k_6, k_7, k_8, and k_9 are the coefficients of $a_{0,2}$, $a_{0,4}$, $a_{1,0}$, $a_{1,2}$, $a_{1,4}$, $a_{2,0}$, $a_{2,2}$, and $a_{2,4}$, respectively, in equation (C12).

REFERENCES

1. Falkner, V. M.: The Calculation of Aerodynamic Loading on Surfaces of Any Shape. R. & M. No. 1910, British A.R.C., Aug. 1943.

2. Runyan, Harry L., and Woolston, Donald S.: Method for Calculating the Aerodynamic Loading on an Oscillating Finite Wing in Subsonic and Sonic Flow. NACA TN 3694, 1956.

3. Zlotnick, Martin, and Robinson, Samuel W., Jr.: A Simplified Mathematical Model for Calculating Aerodynamic Loading and Downwash for Wing-Fuselage Combinations with Wings of Arbitrary Plan Form. NACA TN 3057, 1954. (Supersedes NACA RM L52J27a.)

4. Multhopp, H.: Methods for Calculating the Lift Distribution of Wings (Subsonic Lifting Surface Theory). Rep. No. Aero. 2353, British R.A.E., Jan. 1950.

5. Watkins, Charles E., Runyan, Harry L., and Woolston, Donald S.: On the Kernel Function of the Integral Equation Relating the Lift and Downwash Distributions of Oscillating Finite Wings in Subsonic Flow. NACA TN 3131, 1954.

6. Loving, Donald L., and Estabrooks, Bruce B.: Transonic-Wing Investigation in the Langley 8-Foot High-Speed Tunnel at High Subsonic Mach Numbers and at a Mach Number of 1.2. Analysis of Pressure Distribution of Wing-Fuselage Configuration Having a Wing of 45° Sweepback, Aspect Ratio 4, Taper Ratio 0.6, and NACA 65A006 Airfoil Section. NACA RM L51F07, 1951.

TABLE I

LOCATION AND MAGNITUDE OF WEIGHTING FACTORS TO REPRESENT CHORDWISE LOADING

Chordwise location, percent chord	$G_{0,\nu}$	$G_{1,\nu}$	$G_{2,\nu}$
12.5	0.2734	0.0488	0.0732
37.5	.1172	.0762	.0381
62.5	.0703	.0762	-.0381
87.5	.0391	.0488	-.0732

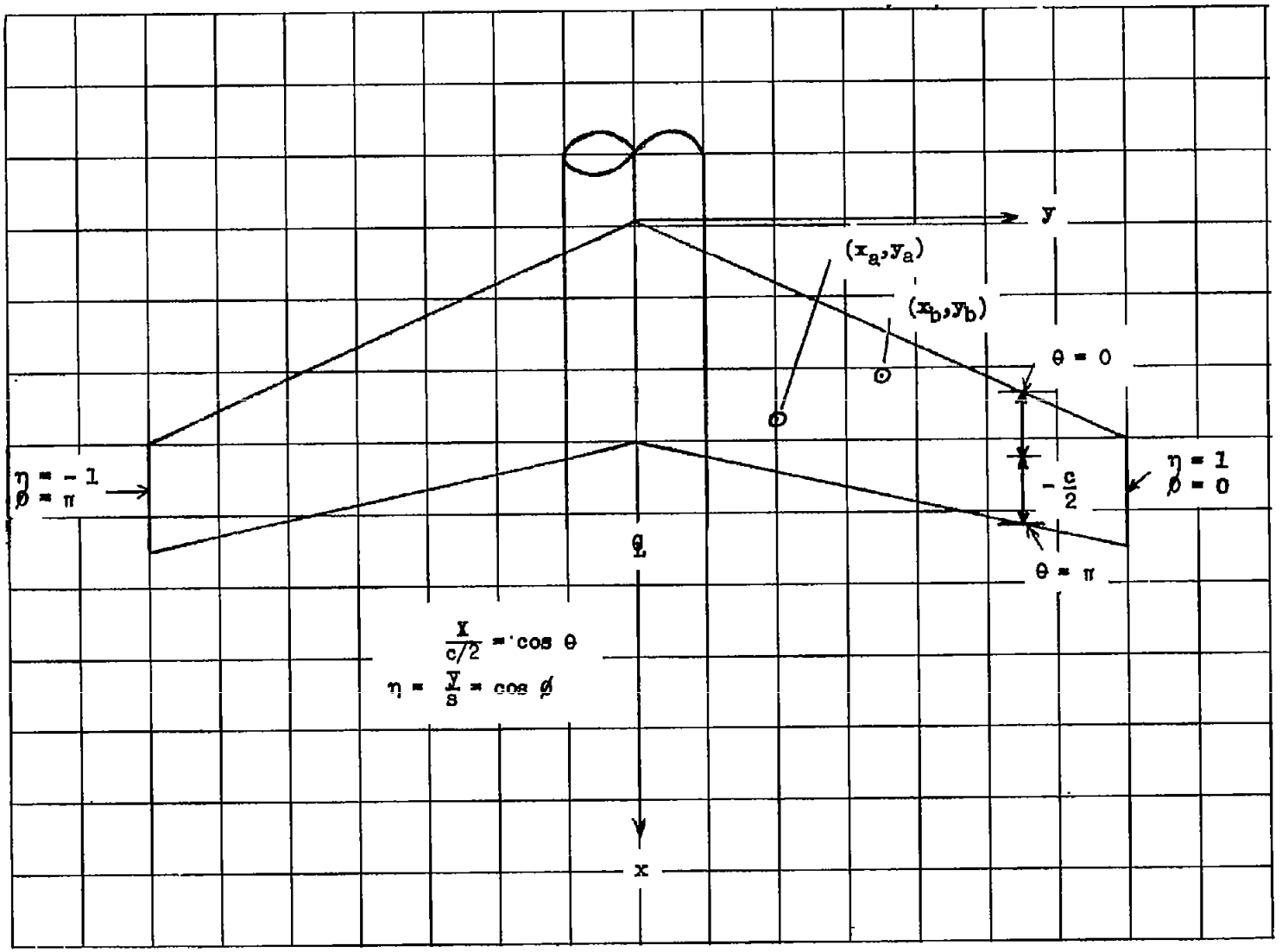

Figure 1.- Wing diagram and coordinate system.

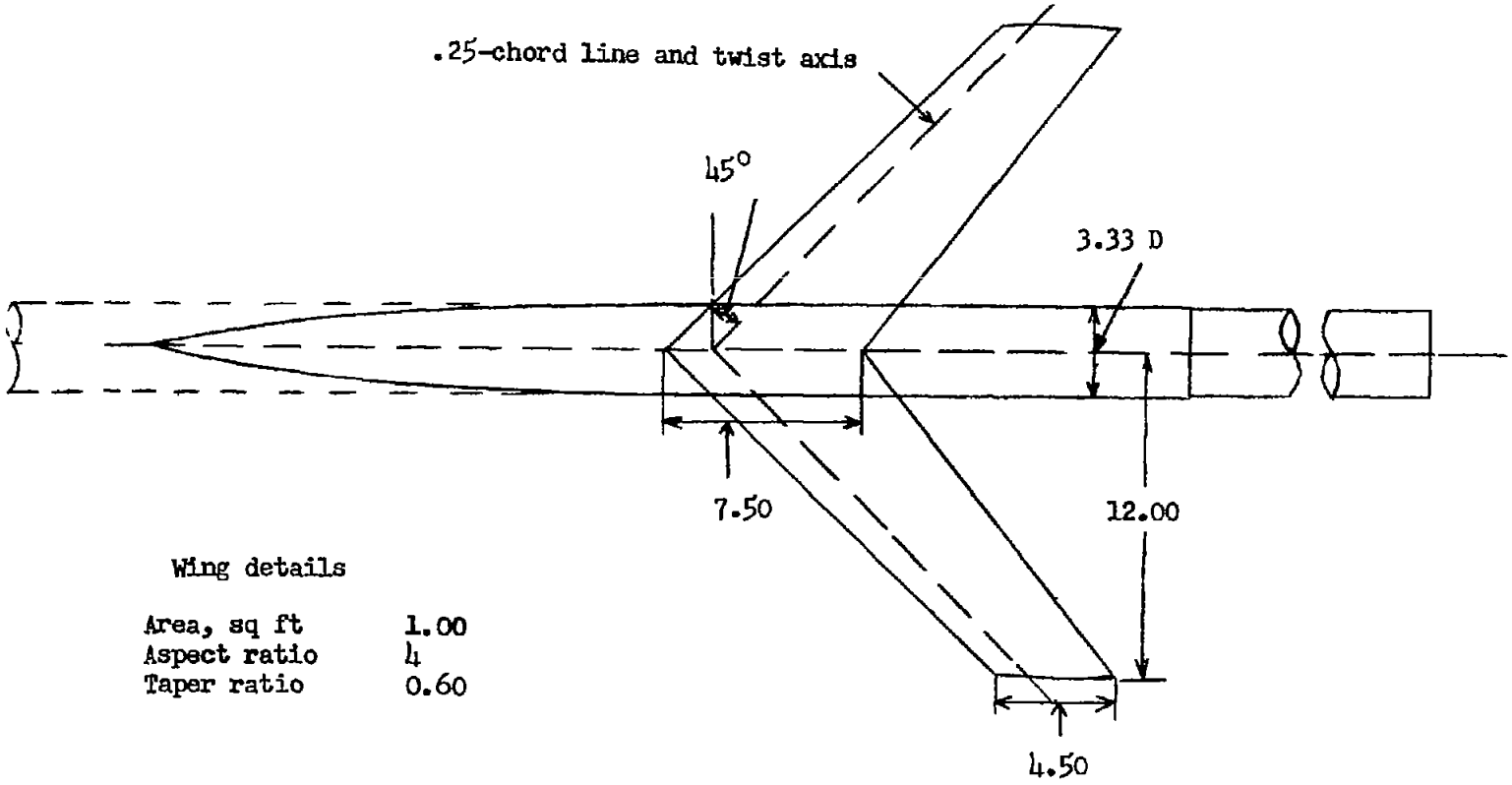

Wing details

Area, sq ft	1.00
Aspect ratio	4
Taper ratio	0.60

Figure 2.- Details of wing-body configuration for wing A. All dimensions are in inches.

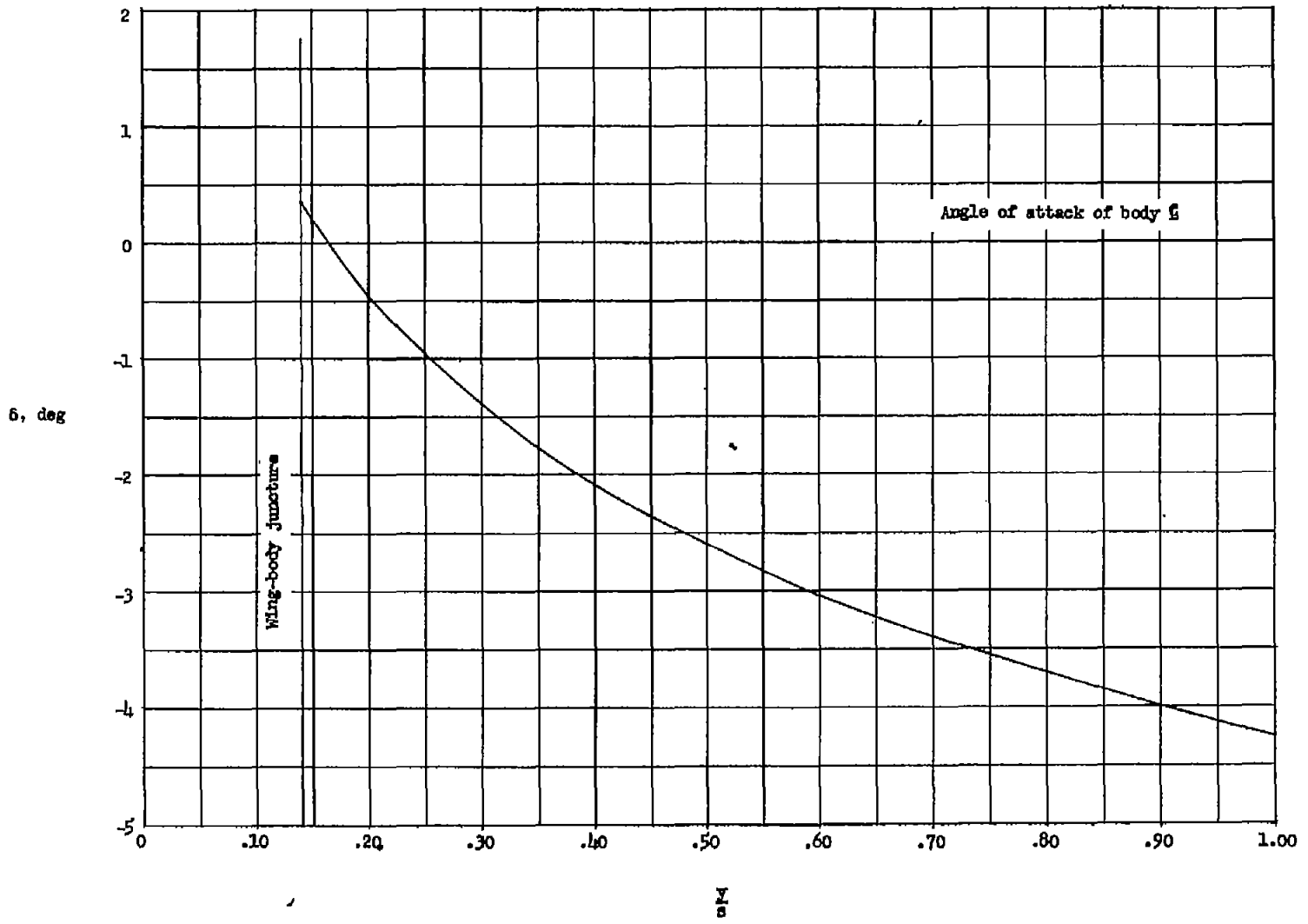

Figure 3.- Spanwise variation of wing twist.

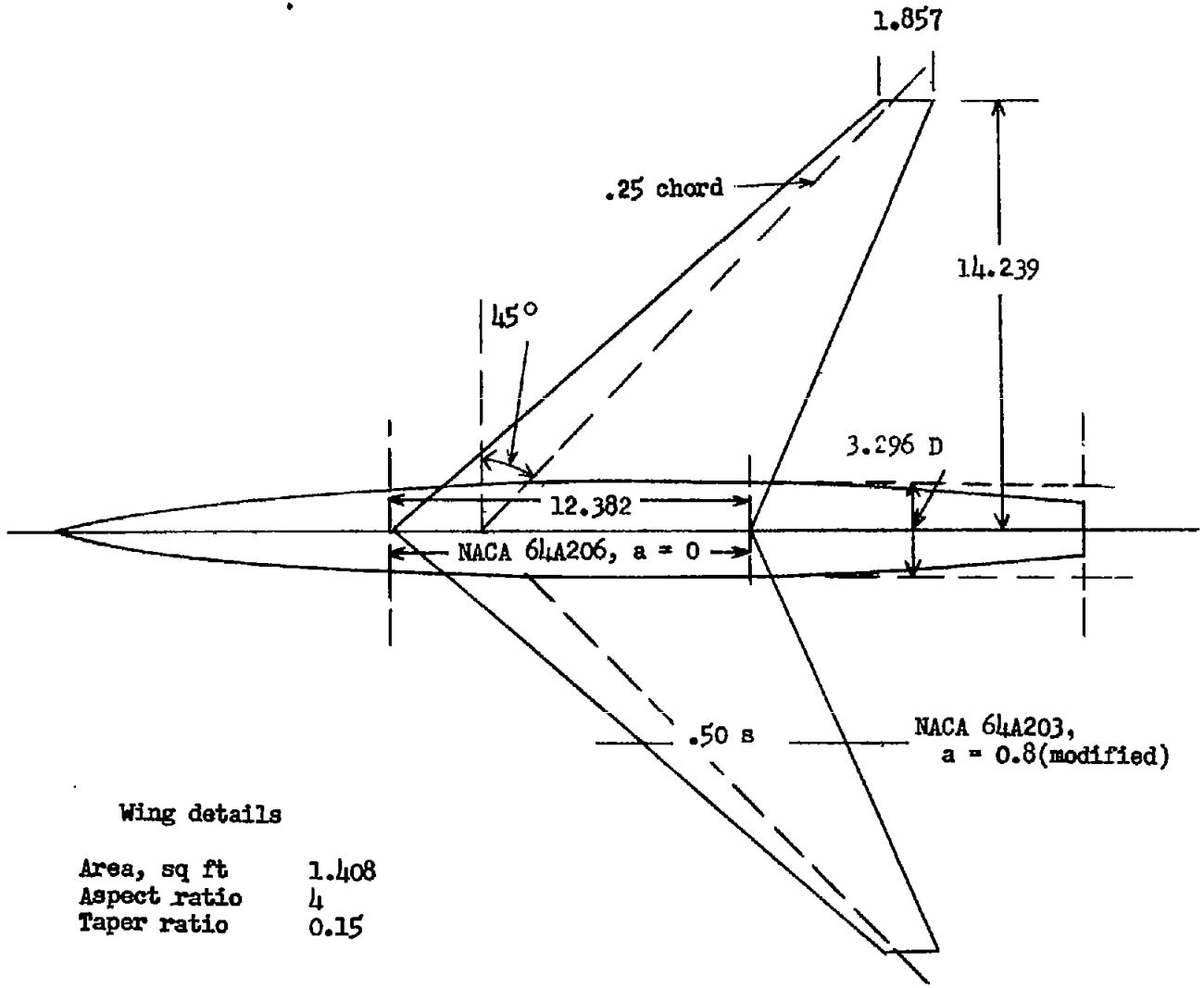

Wing details

Area, sq ft	1.408
Aspect ratio	4
Taper ratio	0.15

Figure 4.- Details of wing-body configuration for wing B. All dimensions are in inches.

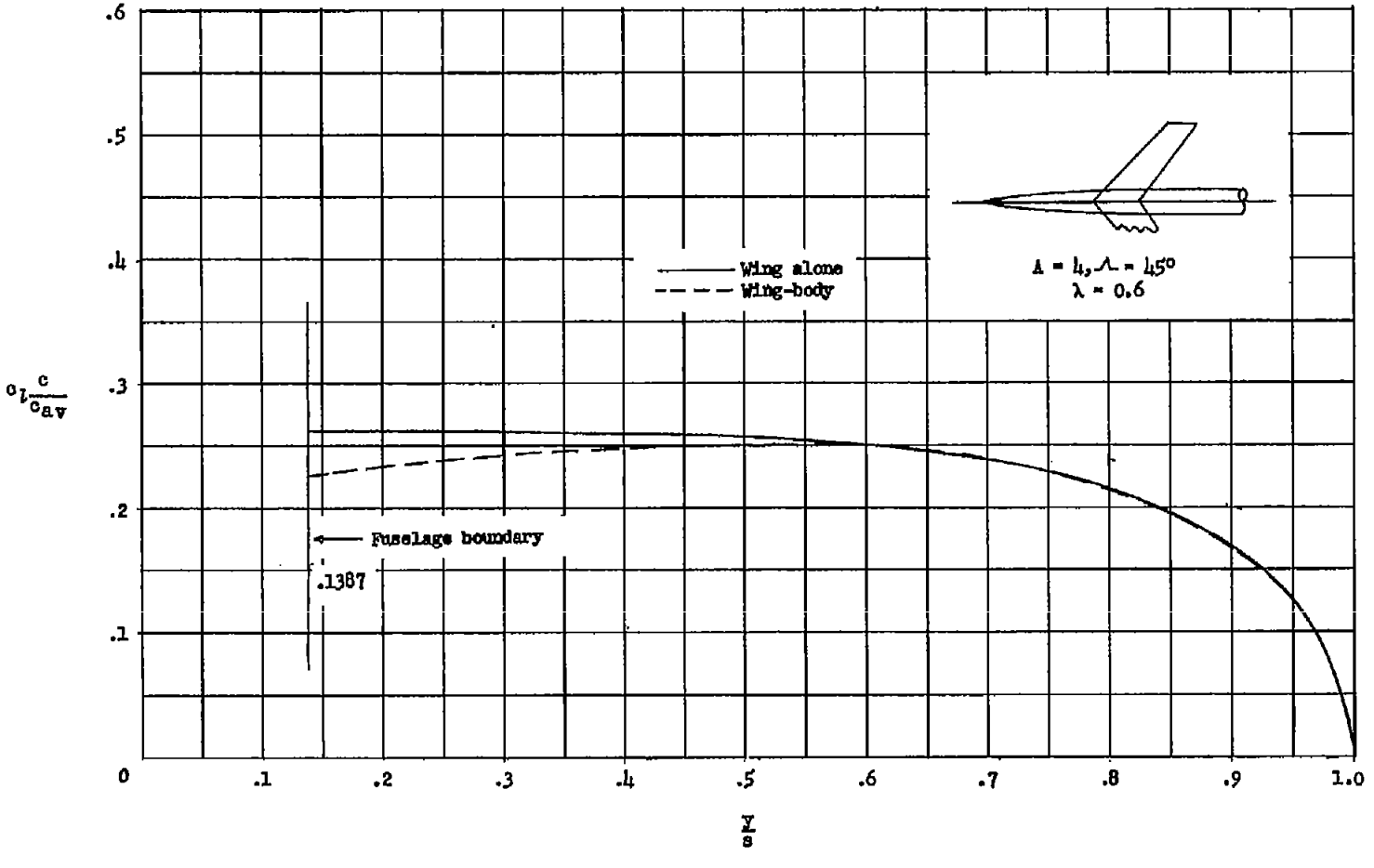

(a) $M_o = 0$.

Figure 5.- Calculated spanwise loading. Wing A; $\alpha = 4.0^o$.

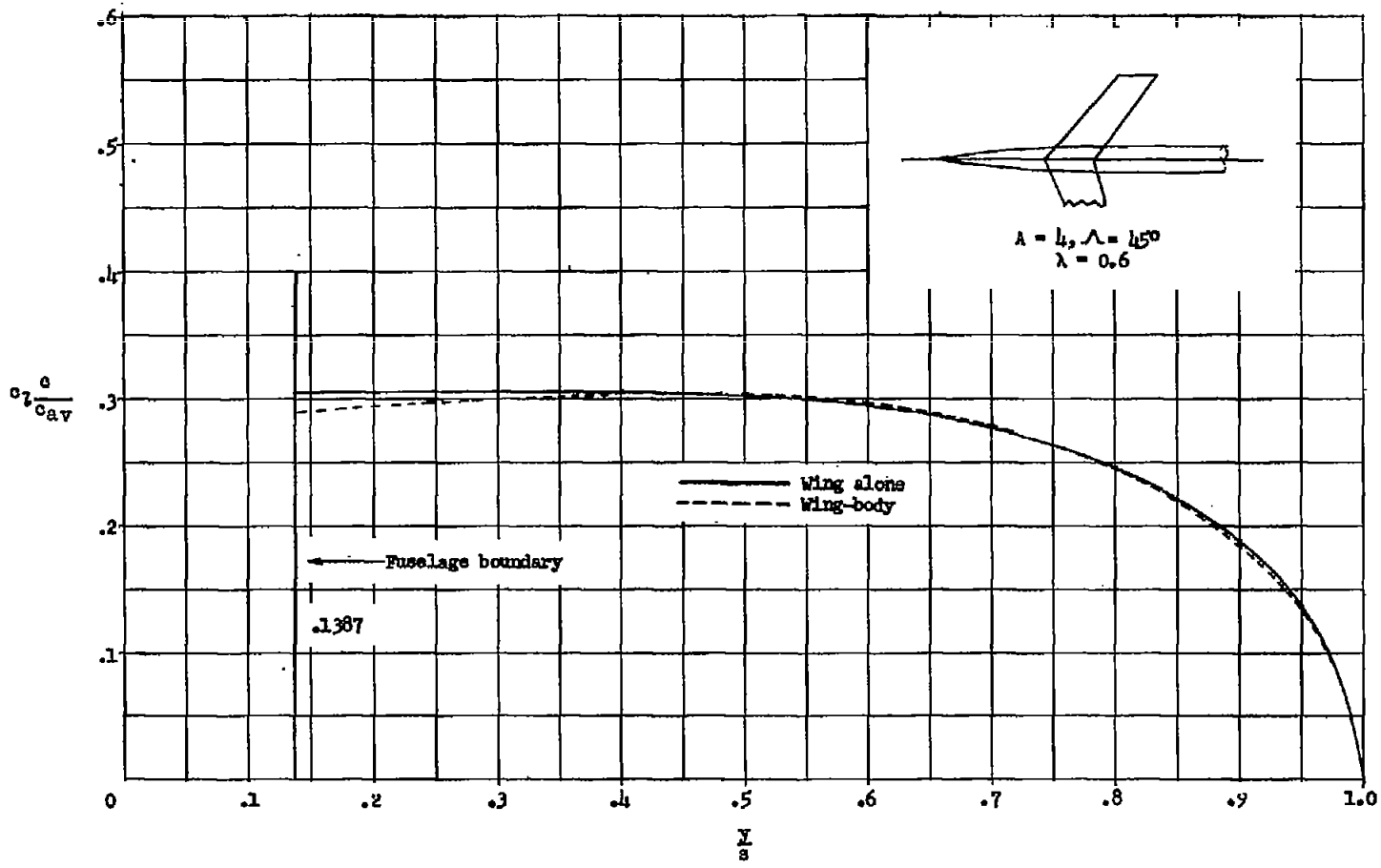

(b) $M_o = 0.9$.

Figure 5.- Concluded.

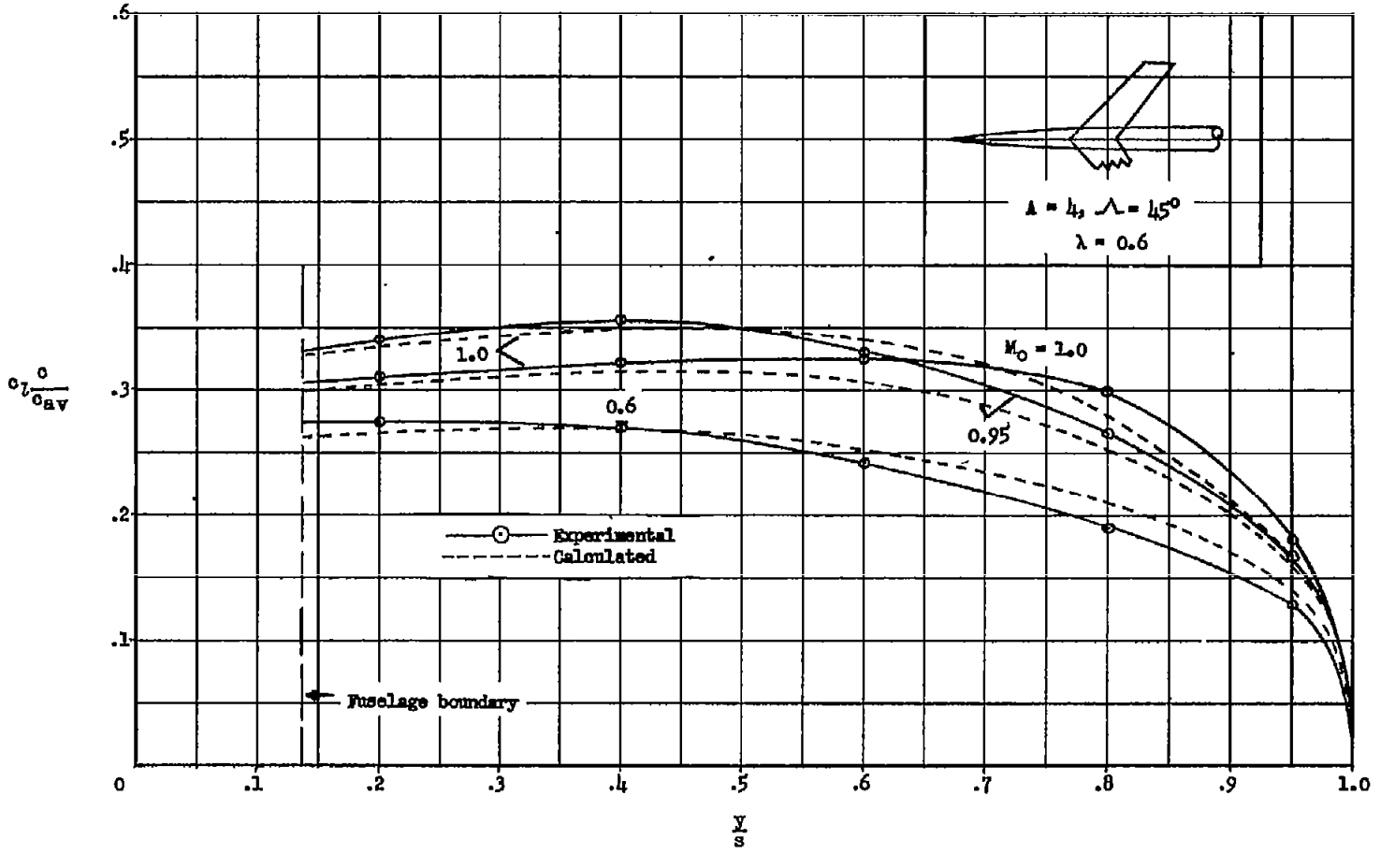

Figure 6.- Comparison of calculated and experimental spanwise loading for wing A without twist. $\alpha = 4.0^{\circ}$.

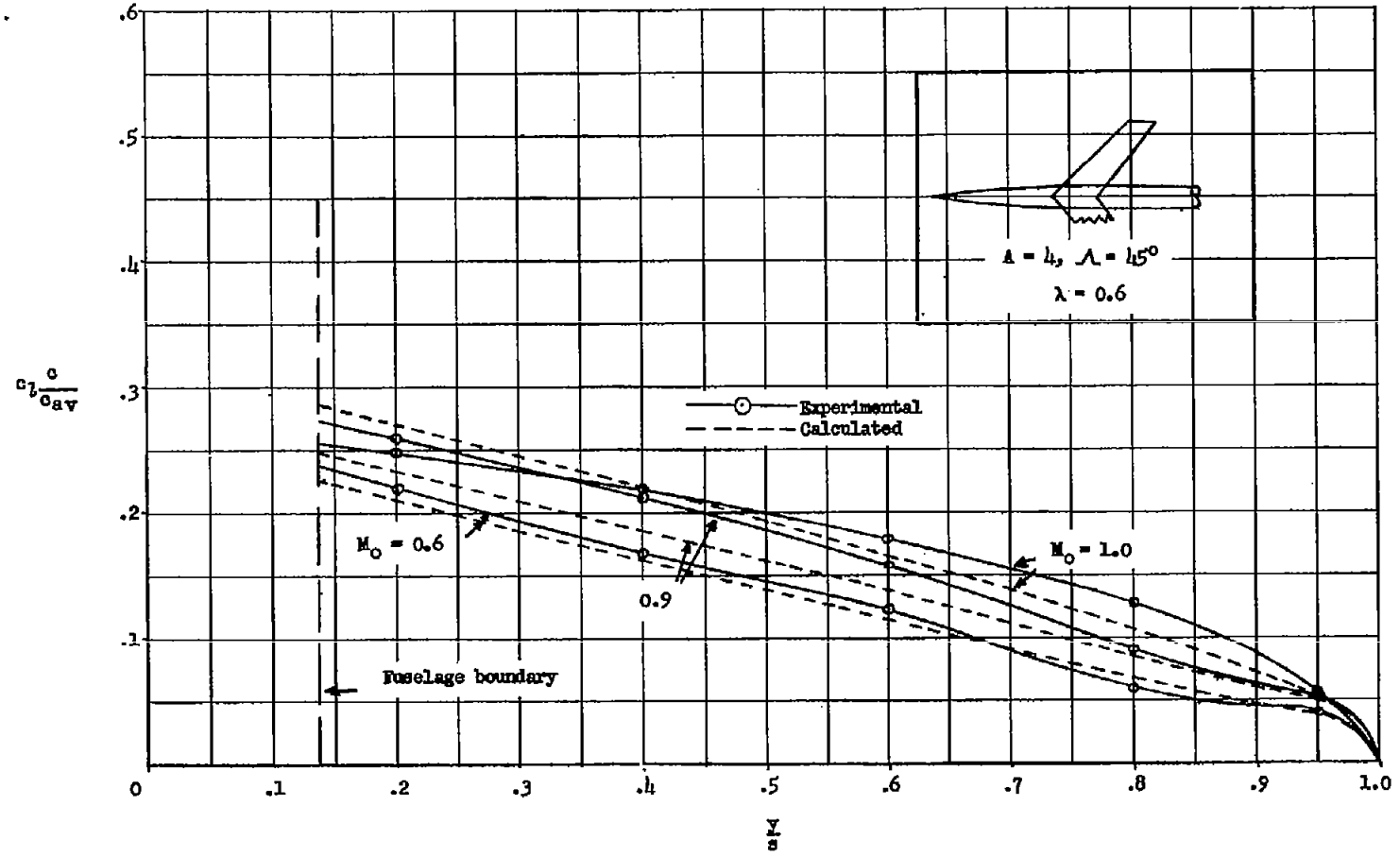

Figure 7.- Comparison of calculated and experimental spanwise loading for wing A with twist. $\alpha = 4.0^{\circ}$.

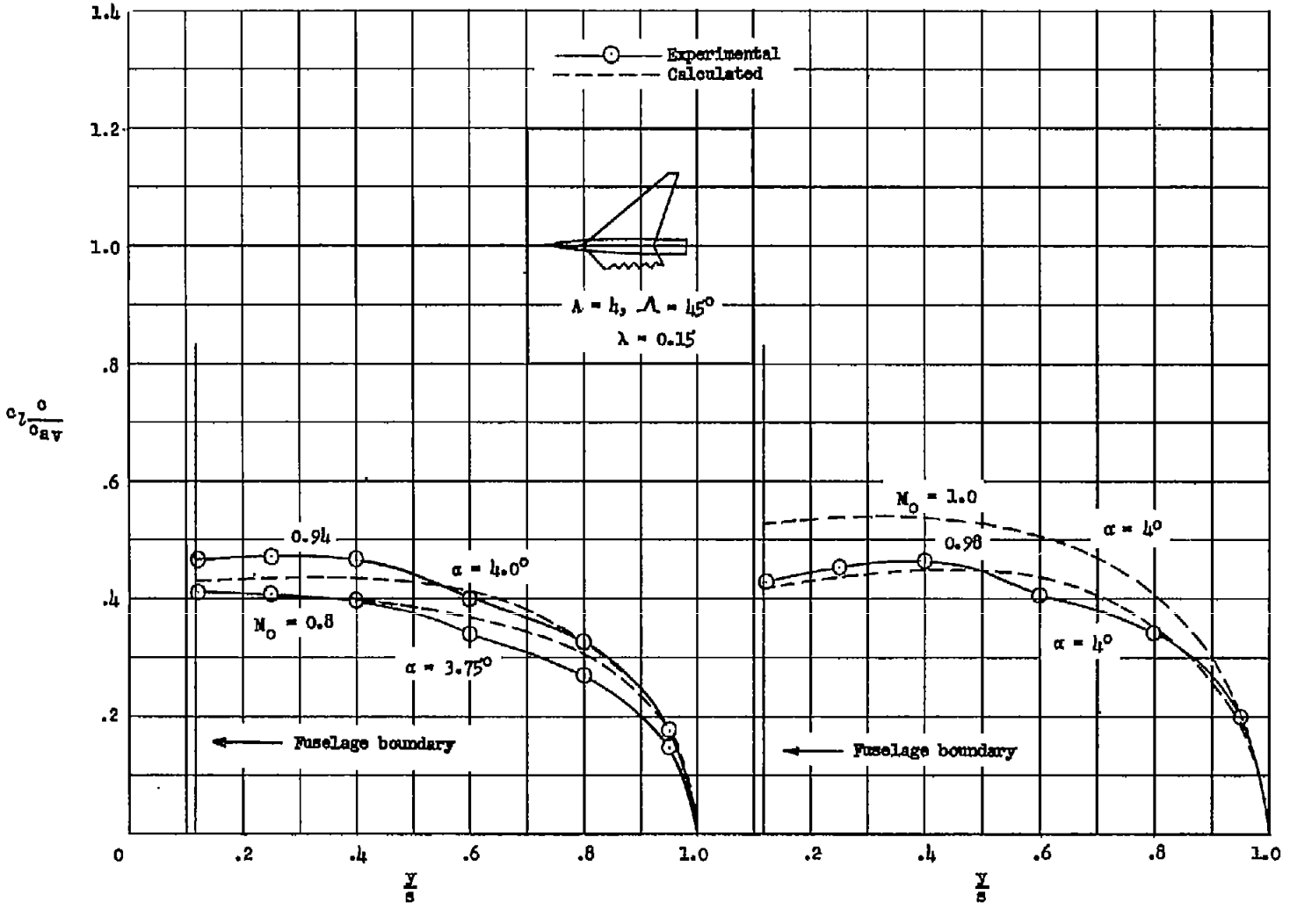

Figure 8.- Comparison of calculated and experimental spanwise loading of wing B.

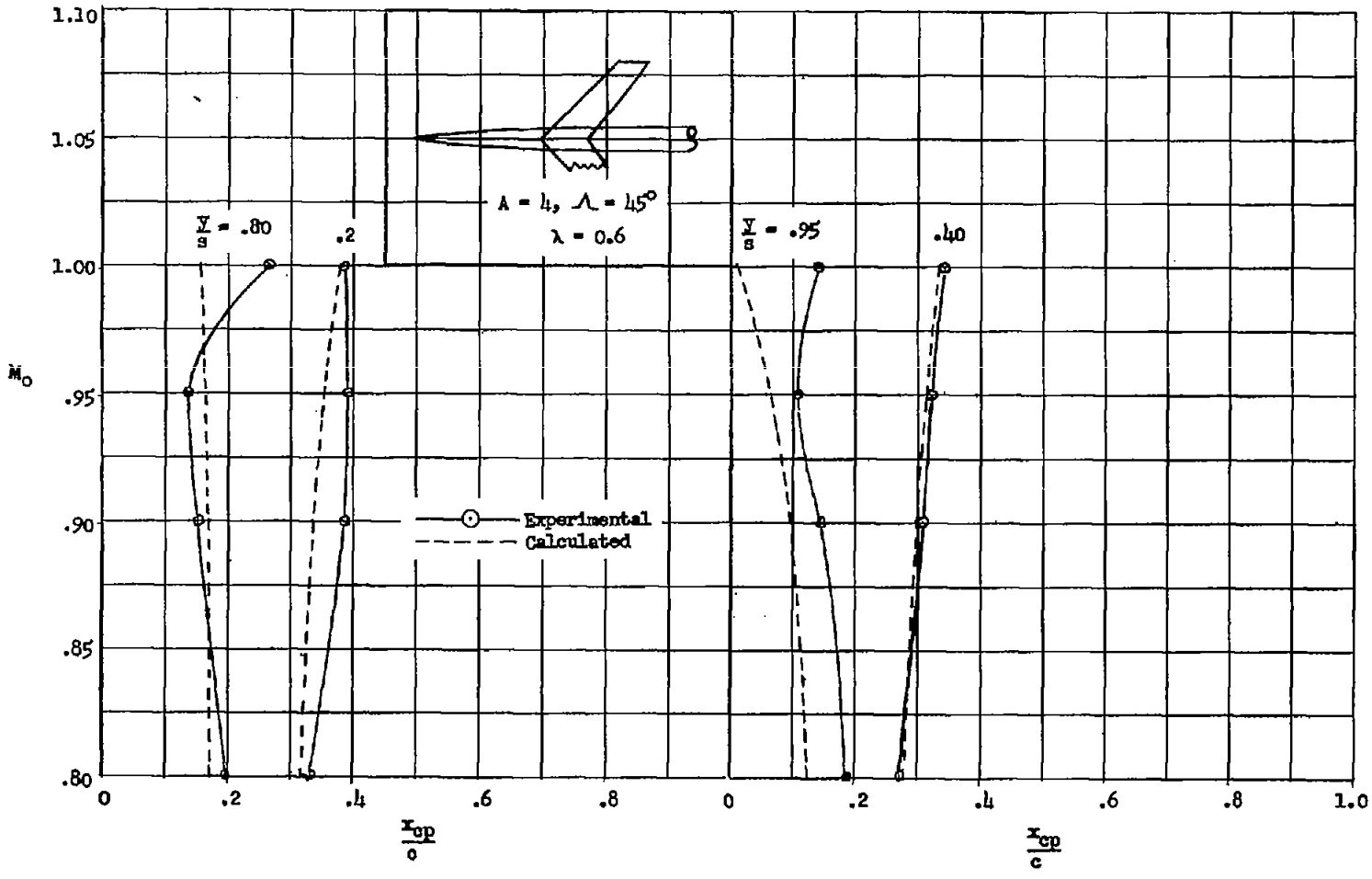

(a) Twist = 0°.

Figure 9.- Comparison of calculated and experimental section center of pressure. Wing A; α = 4°.

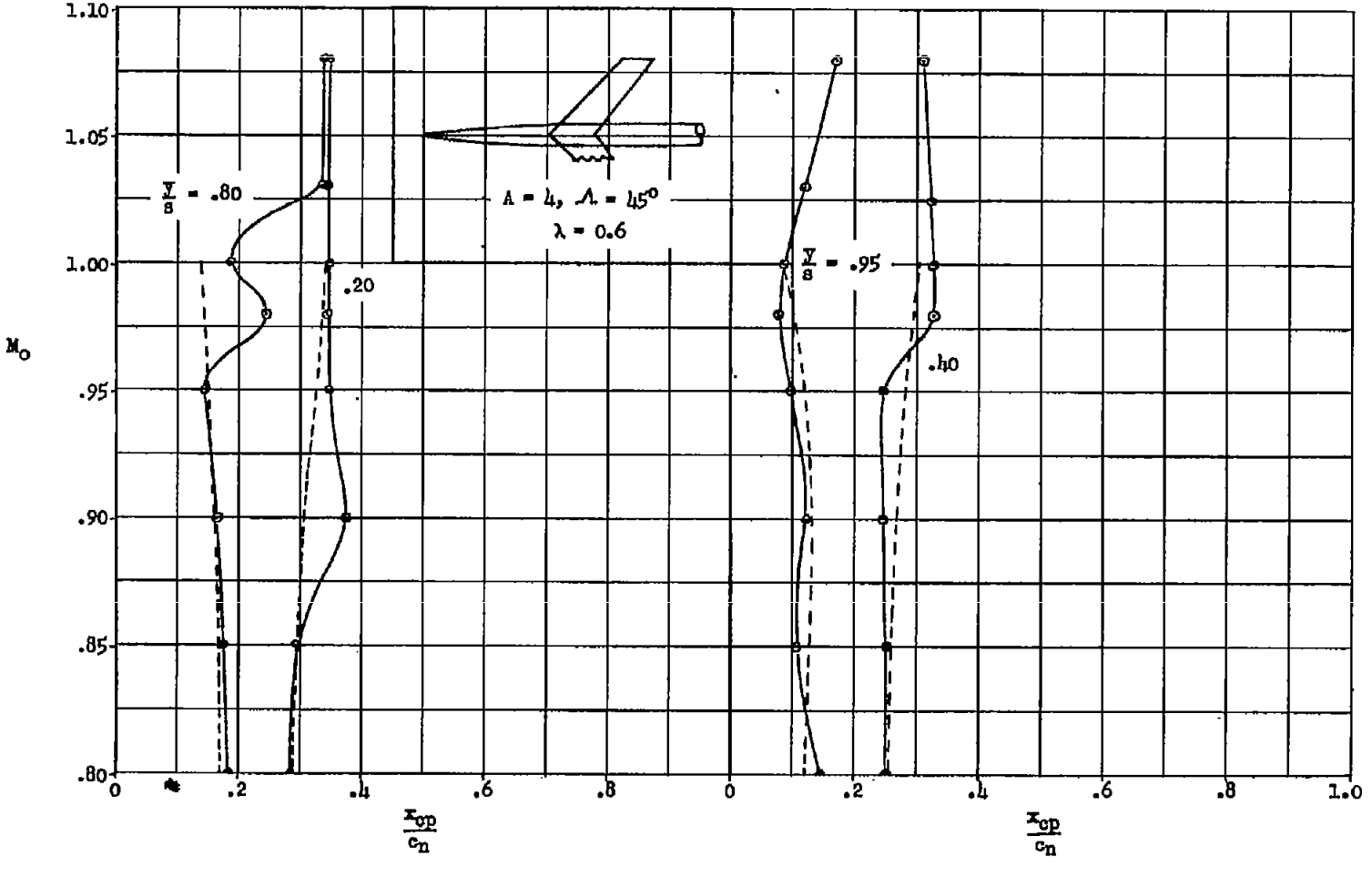

(b) Twist = 4°.

Figure 9.- Concluded.

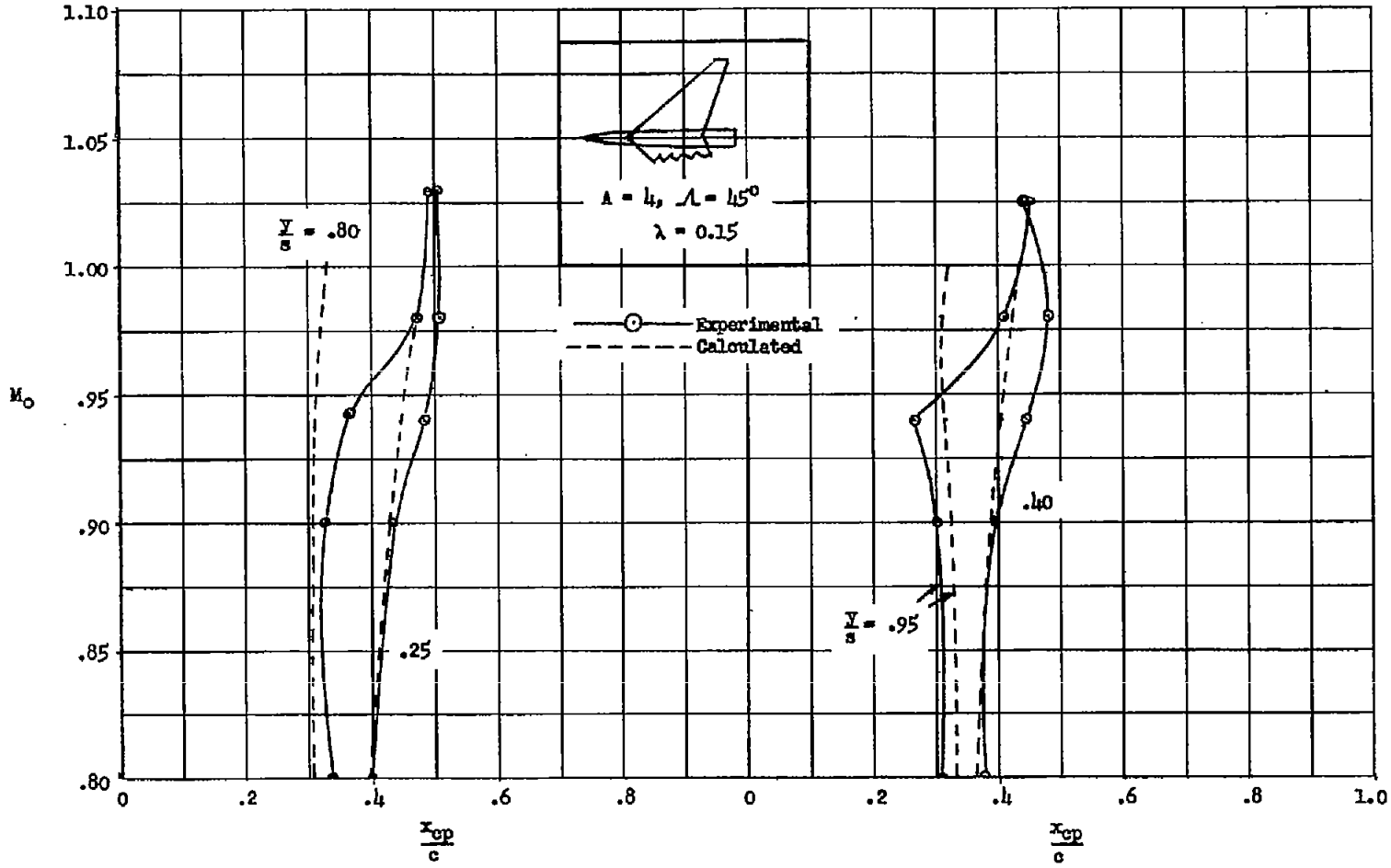

Figure 10.- Comparison of calculated and experimental section center of pressure. Wing B; $\alpha = 4^{\circ}$.

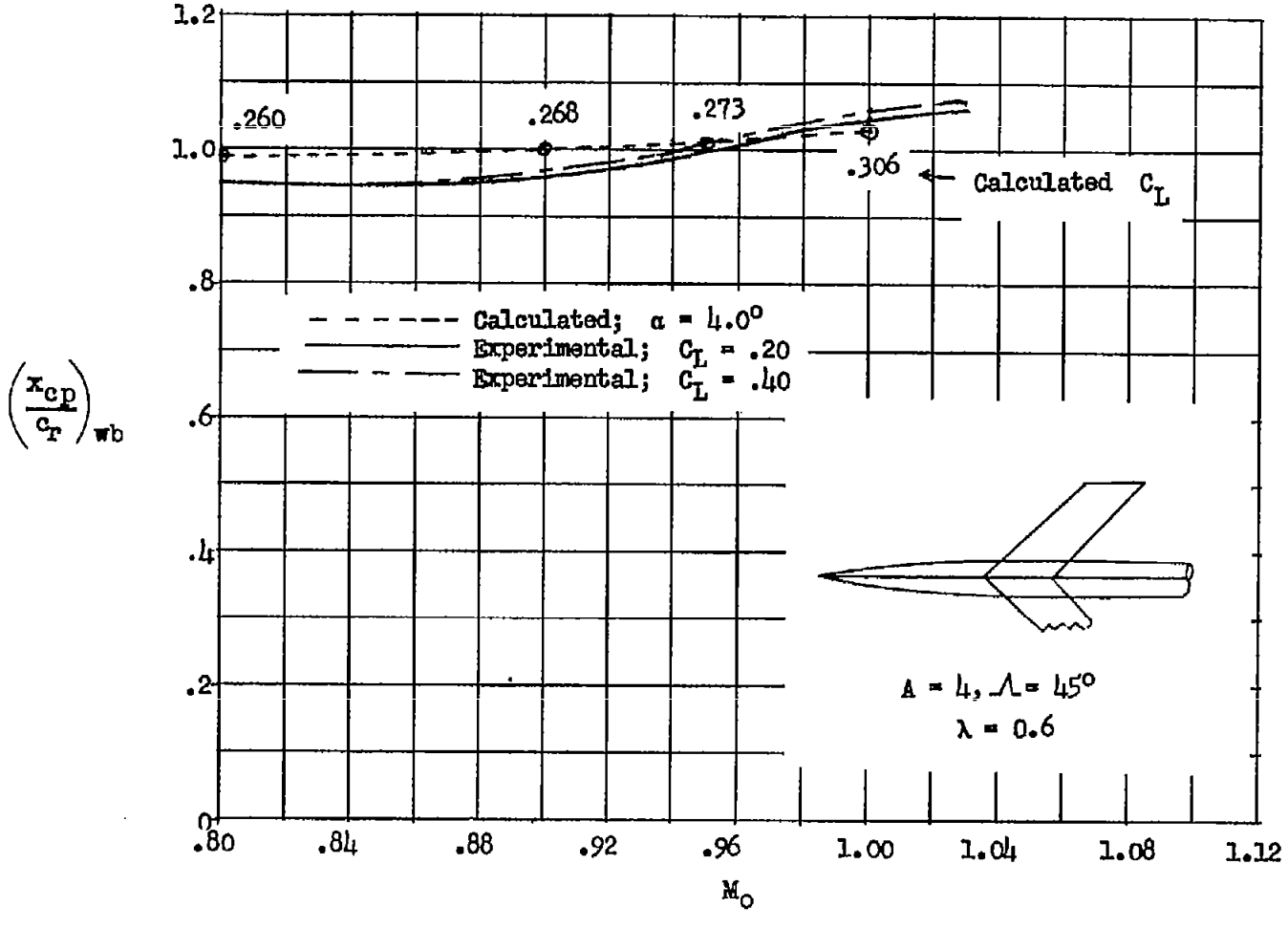

(a) Twist = 0°.

Figure 11.- Comparison of calculated and experimental wing chordwise center of pressure. Wing A.

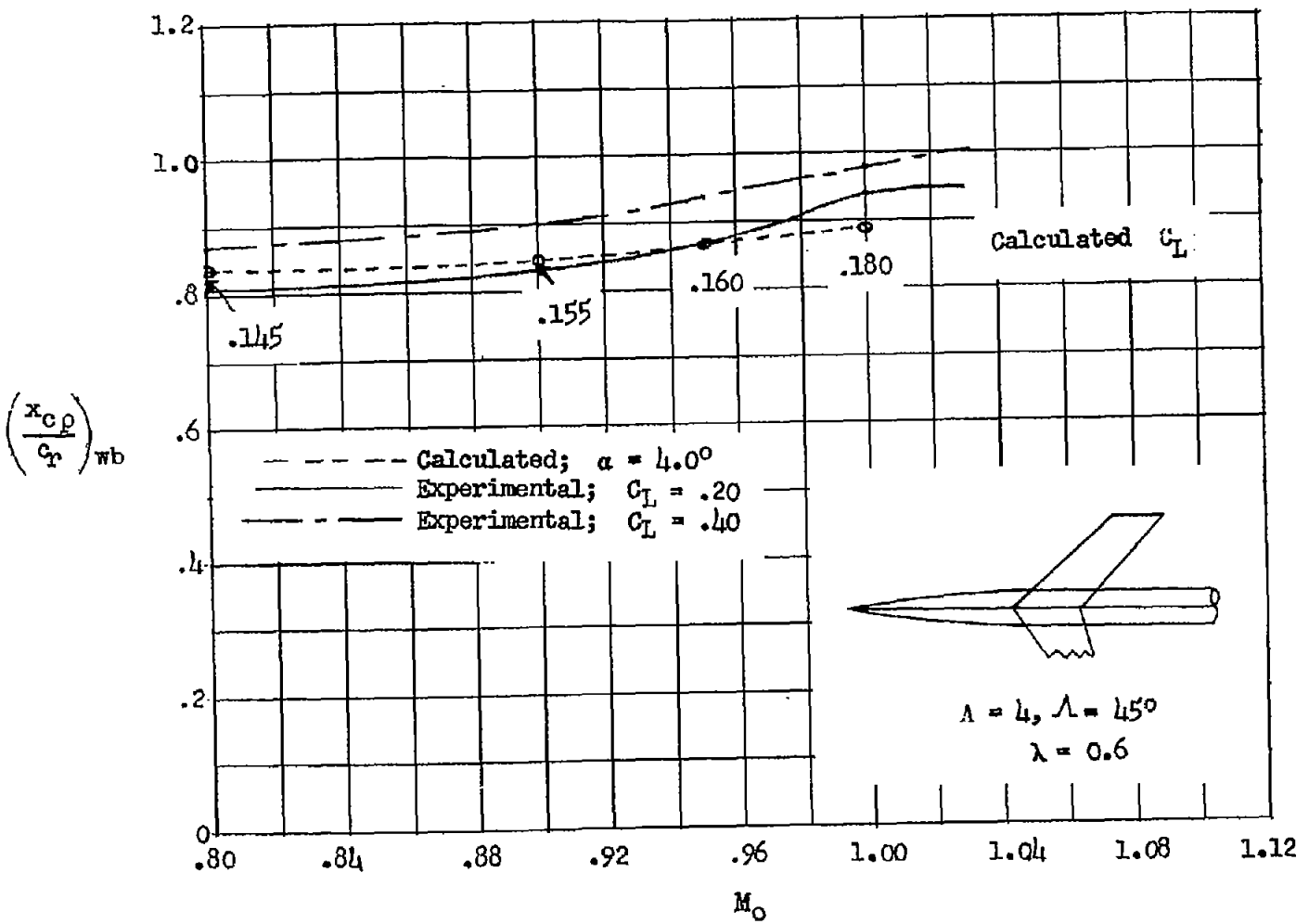

(b) Twist = 4.0°.

Figure 11.- Concluded.

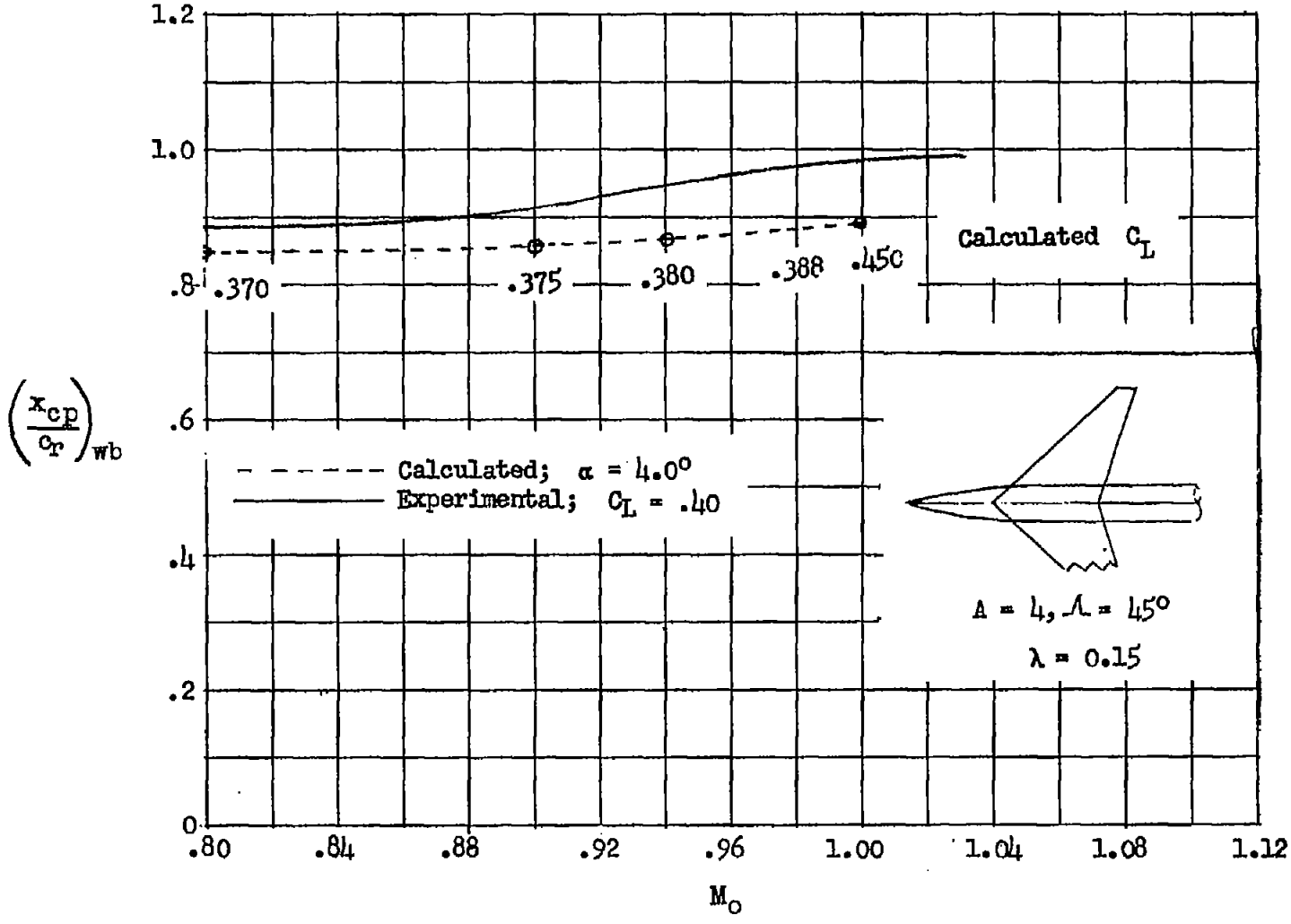

Figure 12.- Comparison of calculated and experimental wing chordwise center of pressure. Wing B.

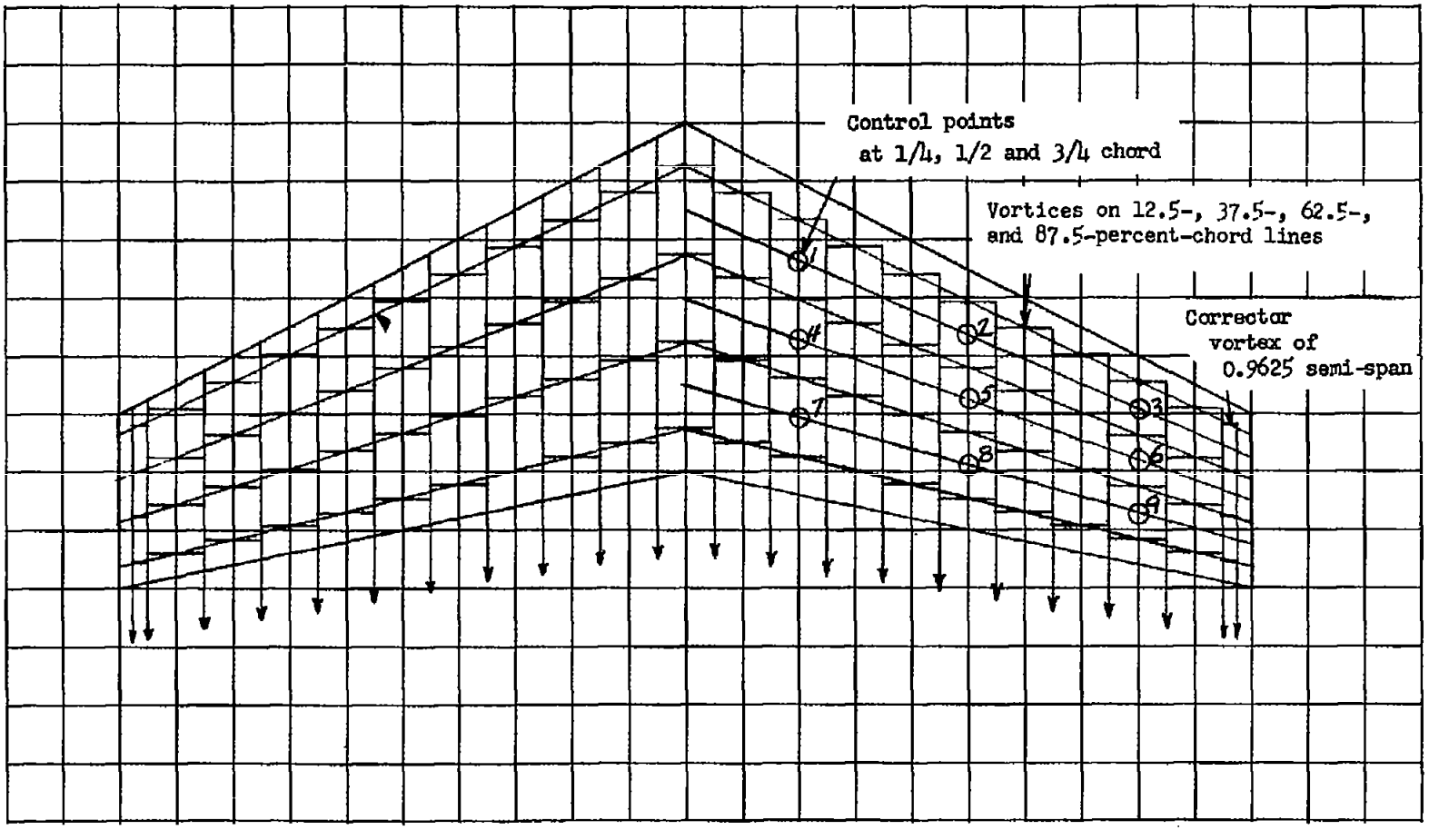

Figure 13.- 84-vortex pattern for wing showing location of nine control points.